Coordination Chemistry Reviews 253 (2009) 575–593

Contents lists available at ScienceDirect

Coordination Chemistry Reviews

journal homepage: www.elsevier.com/locate/ccr

Review

Kohn-Sham DFT results projected on ligand-field models: Using DFT to supplement ligand-field descriptions and to supply ligand-field parameters

Claus E. Schäffer, Christian Anthon, Jesper Bendix*

Department of Chemistry, University of Copenhagen, Universitetsparken 5, DK-2100 Copenhagen, Denmark

Contents

ARTICLE INFO

Article history:
Received 23 June 2008
Accepted 15 September 2008
Available online 25 September 2008

Keywords:
Ligand field
DFT
AOM
Nitrido
Tetrahedral
Vibronic

ABSTRACT

The use of density functional theory (DFT) as a means of providing otherwise inaccessible parameters of ligand-field theory (LFT) is discussed. This application of DFT strengthens both models: it revitalizes ligand-field theory by helping it relieving its permanent burden of over-parameterization, especially when applied to low-symmetry chemical systems, while LFT simultaneously provides a conceptual framework on which the plentiful numerical data from DFT computations can be reduced to familiar values of familiar parameters. The revived LFT contains information that cannot be extracted from DFT, but which, in principle, can be projected back on to DFT, thus providing the complete energy matrix of the partially filled d^q configuration.

Application to two kinds of chemical systems will be described: electronically strongly anisotropic nitride complexes and tetrahedral d^2 systems. In the former applications, focus is on the ligand field, its symmetry partition, and its additivity. In the d^2 systems, the focus is on extracting repulsion parameters, but also parameters of the angular overlap model will be discussed.

Structural and spectroscopic studies corroborated by DFT computations demonstrate that complexes containing the $\{Cr(N)\}^{2+}$ moiety coordinated to weak auxiliary ligands are better considered as perturbed linear systems than axially compressed octahedral systems. Average-of-configuration (AOC) computations on the tetrahedral systems, analysed by using two electronic interaction models, the Slater–Condon–Shortley model and the Parametrical Multiplet Term model, both formulated in terms of mutually orthogonal, barycentered coefficient operators, illuminate two-electron interactions. Thereby the quantitative influence of the individual parameters associated with these operators becomes the novelty of the analysis. The SCS model has D terms and E terms, where D is Jørgensen's spin-pairing energy parameter and E is proportional to the Racah parameter B. The PMT model has four terms, two D terms

* Corresponding author. Tel.: +45 35320101.
E-mail address: bendix@kiku.dk (J. Bendix).

0010-8545/$ – see front matter
doi:10.1016/j.ccr.2008.09.010

and two E terms, and can be used to free the SCS model, which is the superior model for comparing with experiments, from small unwanted parts of the DFT-computational results. For $Cr^{IV}X_4$ in T_d symmetry, the results were as a new illustration deprived of their ligand-field contribution and the remaining "molecular atom" analysed in the PMT model, whereas for the $V^{III}X_4^-$ complexes, distorted to D_{2d} symmetry, the results were described with four PMT parameters, all following the nephelauxetic series, and three AOM parameters, whose computed values provide support to the concept of linear ligation.

Nomenclature

AOC	average of configuration calculation
dppe	1,2-bis(diphenylphosphino)ethane
D	Jørgensen's spin-pairing energy parameter
E	the spatial parameter corresponding to D
$E_{av.}$	average (configurational) energy
GGA	generalized gradient approximation
KS-DFT	Kohn-Sham DFT; KS-orbital or KS-molecular orbital DFT
LDA	local density approximation
LFT	ligand-field theory
LF	ligand field (one-electron operator)
LFR	model encompassing Ligand Field and interelectronic Repulsion
LMCT	ligand to metal charge transfer = electron transfer from ligand to metal
py	pyridine
PMT	H_{PMT} = parametrical multiplet term model. Four-parameter model extending the SCS model of the interaction between the two electrons of d^2 or the pair interactions of $d^q = Q[D_S]D_S + Q[D_v]D_v + Q[E_1]E_1 + Q[E_0]E_0$
$Q[\ ]$	notation of an operator
$Q[D]$	spin and seniority separator, a formal two-electron operator on the full d^2 configuration
$Q[D_S]$	spin separator; operator of Hund's first rule, a formal two-electron operator on the full d^2 configuration
$Q[D_v]$	seniority separator in singlet space, a formal two-electron operator
$Q[E]$	spatial separator, a formal two-electron operator on the full d^2 configuration
$Q[E_1]$	spatial separator within triplet space; operator of Hund's second rule, a formal two-electron operator
$Q[E_0]$	spatial separator within singlet space, a formal two-electron operator
R	interelectronic interaction = interelectronic repulsion (two electron operator)
salen	N,N'-ethylenebis(salicylideneaminato)
SCS	H_{SCS} = Slater–Condon–Shortley model (two-parameter model describing the separation of the five multiplets of d^2 or the pair interactions of d^q) = $Q[D]D + Q[E]E = Q[B]B + Q[C]C$
SSS	sum square splitting
$(SSS)_{PMT}$	$<H_{PMT}\|H_{PMT}> = <Q[D_S]\|Q[D_S]>(D_S)^2$ + etc. = sum of the squares of all the barycentered eigenstates of H_{PMT}
WFT	wave function theory as opposed to KS-DFT

1. Introduction

Density functional theory (DFT) has become an ubiquitous tool in coordination chemistry. It is being applied to increasingly more complicated systems and provides vast amounts of numerical data. This review addresses KS-DFT in its special function as a data source for ligand-field theory (LFT), which has remained for half a century the standard tool for systematizing coordination chemistry. We aim at a consistent and optimal bridge building between the two descriptions, which requires consideration of how the two models are applied.

LFT is a model theory based upon a wave function, quantum-mechanical conceptual framework, but simplified to the extreme. The justification of still focusing on the ligand-field model lies in its glorious history and perseverance: in the fact that LFT was able to take over the rationalization of coordination chemistry after the spd-hybridization model that was associated with such names as Slater and Pauling [1]. After the replacement of the valence bond spd-model, the ligand-field model revolutionized transition metal chemistry by adding the modeling of two-electron interactions that had been developed for d^q configurations of atomic systems by Slater, Condon and Shortley (SCS) [2]. The two-electron interactions represent the interelectronic repulsion (R), and we have named the simplest form of LFT incorporating only the ligand field (LF) itself and the repulsion, LFR [3,4].

LFR had the conspicuous advantage over the hybridization model that it not only covered ground states but also excited states. Thus, the colors of the most numerous class of complexes became understood as caused by weak absorptions of light in the visible region, classified as d–d or ligand-field transitions. In addition, more and more chemical properties could be related to the information that was revealed by these ligand-field spectra. These revelations are well known and can be found in most inorganic texts dated from the early 1960s and up to and including the present time [5]. One of these properties, the ionic radius of a transition metal ion in a complex or in a solid, emphasizes the special character of coordination chemistry, which is characterized by involving central metal ions surrounded by ligands, often placed in a symmetrical way around their central ion. Coordination chemists prefer to conceive their molecular units, the complexes, as consisting of central ions and ligands as opposed to other chemists who conceive individual atoms as their molecular building blocks. A profound chemical reason for this difference has its roots in complexation reactions in solution, which played a dominating part in the development of the subject. This chemistry was always classified by the central ions, which were attributed an ownership to the ligands, which carried the variation for a given central ion [6].

The idea of a central ion is of course derived from the mathematical concept of a sphere, which is associated with the orthogonal concepts of radial and angular, concepts that are as central for LFT as for coordination chemistry in general. Actually, when we call LFT semi-empirical, we do so because only the angular part is theoretical. The radial part is empirical since it is derived from the optical spectra and/or other experimental data and for each chemical system individually. The central point of the present review is the methodology involved in using DFT to compute this radial part of LFR.

Initially quantum chemists did not take LFT seriously because of the enormous simplifications on which it was founded. However, as computational chemistry became surmountable, it was soon realized that all the many numbers that came out of this kind of

activity needed a chemical vocabulary in order to become communicable. Even though we are coordination chemists, it was still this way of thinking, which was one of our driving forces when we tried to approach LFT computationally. We owned an edifice based upon useful concepts, but the question was: how stable were these concepts? Another driving force was a consequence of two coupled computational developments. The Hartree–Fock–Slater model, also called the Xα-model, had been used successfully from the early 1970s and had gradually evolved to the Kohn-Sham DFT model with a strong foundation in theoretical understanding and practical experience. Moreover, computational packages had become available for the use by everyone, and DFT had already established itself as a useful tool for the coordination chemist.[1] Time-dependent DFT will not be considered here since it has severe limitations in applications to certain systems containing LF multiplets [7].

Our focus when we wanted to try to approach LFT computationally was the involvement of DFT in the problem of the interelectronic repulsion. It seemed to us that the strongest test of the general usefulness of DFT in mimicking LFT would be its ability to handle the interaction between the individual electrons in view of the fact that DFT fundamentally is based upon the total electron density [17]. This density is only very indirectly influenced by the question of how the probability densities of two electrons depend on each other and it is a counterintuitive idea that this question should be related to the total electronic density distribution!

A semiempirically based ligand-field concept, named nephelauxetism, puts an emphasis on the reduction in the energy parameters describing the observed interelectronic repulsion in complexes as compared with those known from atomic spectroscopy of the corresponding atomic ions [8,9]. Jørgensen proposed two rather different explanations for the nephelauxetic phenomenon. The first explanation was *a ligand-field explanation*, which already had been implied in the word nephelauxetism: an expansion (growth) of the electronic cloud of the d electrons. Jørgensen accordingly named LFT the expanded radial function model. Jørgensen then argued that this cloud expansion was due to screening of the central ion nucleus by charge transfer from the ligands to the central ion. That is, s- and p-covalency [10].

The background for Jørgensen's second explanation came from the fact that the coordination chemists, and, in particular he himself, had empirically realized that LFT was too simple and resulted in too many paradoxes to be a true picture of the world of coordination chemistry. Moreover, even though LFT was a quantitative theoretical model, it still contained semi-empirical quantities in the form of its empirical energy parameters. Therefore, the qualitative molecular orbital explanations, which the physicists (van Vleck) [11] had early on allowed to creep into the ligand-field framework of explanations of everything in this part of science, became an indispensable qualitative superstructure to LFT, and with the added explanations of the expanded radial functions, a name was lacking for the simple, but quantitative original ligand-field model. Therefore, we proposed the name, the Parametrical d^q Model, for quantitative and completely well-defined LFT [3b].

Jørgensen's second explanation of nephelauxetism went a bit further away from quantitative LFT. He said that nephelauxetism might be a dilution of the d orbitals that could be understood in the LCAO-MO description of the bonding: the partially filled orbitals, which were treated as neat d orbitals by quantitative LFT, contained ligand orbitals as well. That is, d-covalency [10].

The question of whether s- and p-covalency or d-covalency can be simultaneous or alternative explanations of the nephelauxetic phenomenon has now been an open one for 50 years. The upcoming question then was whether or not DFT would be able to energetically mimic the Parametrical d^q Model as a whole, LF and *R*, for any number of d electrons in the partially filled shell and include a discrimination between the two explanations of nephelauxetism. Ideally, we even wanted to see a quantitative discrimination between them. Moreover, we found for the chemical systems discussed in Section 4 of this review, that the nephelauxetic series could be reproduced in two different ways, which pointed in the direction of both of Jørgensen's mechanisms without being able to quantify their relative contributions [4].

While ligand-field theory is quantitative in most of its formulations, the full advantage of a symmetry-based model is only realized when the assembly of LFR operators are also strictly symmetry based. This approach led to the introduction of the orthonormal operator's formalism, based on the concepts of operator orthogonality and norms. While this formalism could be employed instead of more traditional formulations of LFT in all practical applications, it only obtains its full beauty and simplicity when applied to full d^q-configurations. As always, the lack of complete experimentally observed such configurations then is an obstacle. However, with DFT as a "data source", we can carry out analyses employing a well-defined partitioning of LFR by using parametrical operators that are orthogonal and thereby result in uncorrelated parameters.

In this context it is noteworthy that the LFR model consists of a sum of two barycentered terms, the ligand field term LF with the molecular symmetry and the repulsion term *R* with spherical symmetry. Moreover, all the theory of LFR is buried in its angular factors whereas the magnitudes and signs of the radial factors have to be determined by comparison of theory and experiment. This is where DFT comes in, providing a similar, but not identical, kind of information to that of spectroscopy, that is, information about the radial parameters. The consequences of the symmetry features of LFR are that once *q* of d^q is known, then the angular part of *R* theory is fully determined. Once the molecular symmetry is known, the holistic or non-additive LF theory is also fully determined [3,48], and once the geometry is known, the AOM parameterization is determined and can be used as an additive model [52].

The review is organized as follows: in Section 2 we briefly review the conceptual background of our approach to computation of LFR parameters by DFT. In Section 3 we describe the simplest situation possible within LFR, namely d^1-systems for which the *R* part disappears. This case will be exemplified by high-valent nitride complexes, mainly of chromium(V). The discussion will be supplemented with a few comparisons with their manganese(V) analogs, which by being d^2 systems represent the simplest cases for studying the description of the *R* part of LFR by DFT. We conclude Section 3 by introducing a method for extending the scope of the mapping of AOC-DFT upon the LF by extension to linear vibronic coupling coefficients, a method which aids in relieving the over-parameterization in the description of the ligand field. In Section 4 we dissect the interelectronic repulsion while examining a range of tetrahedral d^2 systems and their parametrical results. In Section 5 we conclude with a few comments on the possible symbiotic future of DFT and LFT.

This review is mainly concerned with our own previous work. However, only a few authors have taken up the challenge to confront the two apparently non-commensurable theories, DFT and LFT. Therefore, we shall mention the resemblances and differences between their work and ours at appropriate places in our text.

[1] Note that we will from here on in general use the term DFT to denote KS-DFT, or where applicable spin-unrestricted KS-DFT, unless the orbitally based nature of KS-DFT needs to be emphasized.

2. Methodologies for bridging between DFT and LFT

Kohn-Sham DFT has its orbitally based formulation in common with LFT. By their common approach to building many-electron bases from their orbital fundaments, these models lend themselves to being used for mutual illumination. The relationship between DFT and LFT has been investigated and elaborated during the successful entry of DFT as a popular tool in coordination chemistry: early efforts focused on making a correspondence between DFT and LFT via commensurable orbital splitting patterns obtained by the two methods [12]. We have used this simplest of translations from DFT to LFT in our studies of nitride complexes of the first row transition elements. The results of these studies are reviewed in Section 3 of this paper.

A more general correspondence between the two models is established when also modeling of interelectronic repulsion within the partially filled shell is included [17,22,4]. The first general approach to this type of correspondence where the energies of the many electron eigenstates are calculated from a sufficient number of computations representing what in wave function theory (WFT) would correspond to the expectation values of the energies of Slater determinants was introduced by Ziegler et al. [13]. The resulting "single Slater-determinant energies" were subsequently translated into eigenenergies by solution of a set of linear equations [13]. On this basis, the basic scheme for mapping DFT data onto LFT was at hand. However, an adaptation to LFT was required in order to make schemes that were generally useful. Further development of the method to include orbital degeneracies was made by Daul [14] who attempted to obtain expressions for the energies of the multiplet terms of d^2 in terms of those of the Slater determinants mentioned. However, this work was not completely successful since its energy expressions for the singlets contain determinants with $M_S = -1$. Later, when the method was further developed, it suffered from an arbitrary selection of its Slater determinants, the only requirement being that they were sufficient as far as their number was concerned and their energies parametrically independent. By this procedure any systematic error in the DFT functionals could devaluate the results.

We constrained KS-DFT by using the so-called average of configuration, AOC-DFT [16,17], which for atomic systems corresponds to a spherically symmetrical Hamiltonian [4] conventionally also used in quantitative LFT to mimic the energies of the multiplet terms of d^q configurations. Thereby, we found that from a symmetry point of view, there were not only accidental errors in certain AOC-computed Slater-determinant energies, but also systematic deviations from the Slater–Condon–Shortley model [17]. Therefore, we used the complete set of Slater-determinant energies and the associated data reduction in order to mimic the SCS model optimally. The least squares procedure used for this purpose had the additional advantage of its statistical machinery, which delivered the residual of the variance and the associated standard deviations on the fitted parameters. Thereby, in addition to avoiding the arbitrariness in the choice of Slater determinants, we now had a well-defined standard method for a detailed analysis of the strengths and shortcomings of the particular complete KS-DFT model on d^q as to its ability to mimic the *R* part of LFR.

We used DFT to study atomic d^q systems using the parameterization methods of the atomic spectroscopists [54–56]. Two different interelectronic repulsion models for d^q were used, the conventional Slater–Condon–Shortley model, where the energies of Slater determinants are described by exchange and coulomb contributions exclusively, and the Parametrical Multiplet Term model [4] where electronic correlation with configurations outside d^q can be partly modeled as well. The PMT model for d^2 was previously denoted PMT[d^2]. This model is a complete d^2 model in the sense that it mimics the multiplet term energies of the d^2 configuration exactly [20]. The Parametrical Multiplet Term Models for d^q for varying *q*, PMT[d^q] ($q = 2, 3, \ldots, 8$), were used in the past to obtain one-electron spin–orbit coupling parameters for all the atomic systems for which complete sets of *J* levels had been obtained experimentally by the community of atomic spectroscopists. The PMT model has the advantage that the residual variance after the multiplet energies have been determined should contain information about the spin–orbit coupling only. We have tried to take advantage of the same idea in our attempts to mimic the LF part of LFR. We want to emphasize that the PMT models are spherically based like the SCS model and, in addition, that the PMT[d^2] model may be used to eliminate systematic errors of the sets of functionals we have used [4].

Atanasov and Daul extended our work on atoms by adding more d^q systems and by including all the f^q systems, but still using the SCS model [15d,15e] and its conventional parameterization. They extended their analysis of the AOC-DFT computational results and went beyond the usual determination of empirical parameters from computed energies by adding the use of the KS-DFT orbitals to calculate the SCS- and the Racah-parameters of the SCS model.

The AOC-DFT computational scheme was also employed by us for molecular ligand-field systems exemplified by the tetrahedral VX_4^- and by inspiration from Atanasov and Daul [18b,18c], we included the CrX_4 (X = F, Cl, Br, I) systems, which have the advantage of carrying no external charge. A comparison of the results of these applications with special focus on nephelauxetism and AOM parameterization will be reviewed in Section 4.3 of this paper.

Atanasov and Daul have developed the LFDFT model, which is mathematically equivalent to our way of establishing a relationship between KS-DFT and LFT. They also use the AOC-DFT model [18] and the complete set of Slater determinant energies. Moreover, they have extended their work to include spin–orbit coupling, f^q configurations and exchange interactions within polynuclear complexes. Even though we thus use the same way of modeling, we find it worth while to emphasize that we, on the one hand, are concerned with a complete molecular KS-DFT model for which KS-DFT orbital and single Slater-determinant energies are obtainable and, on the other hand, a conventional ligand-field model, which is complete within d^q and therefore, in principle, includes some of the near degeneracy correlation because it allows the complete energy matrix on d^q to be obtained. In our opinion the most important fact up until now is that the two models are connected by a one-to-one relationship between the orbitals as well as the Slater determinants of the partially filled shell, but this shell is the only point in common between the molecular AOC-DFT and conventional atomic LFR. Of course, there exists a superstructure to LFR, which qualitatively connects the two models also beyond the partially filled shell, but this is a completely different story which has not yet been explored in any detail (see Ref. [4], Fig. 5, p. 288).

Atanasov and Daul's use of LFR is conventional and thereby different from ours, which use a formulation of *R* in terms of coefficient operators that are orthogonal so that the parameters are independent of each other and can be determined one after the other. Moreover, the individual effects of these operators on the energy splitting of d^q is then a concept which can be easily quantified. In Section 4.2 we shall discuss our orthogonal operator's results for CrX_4 (X = F, Cl, Br, I).

In the orthogonal operator's formulation of LFT [3,4,6,17,19], the Parametrical d^q Model is written as a sum of conglomerate operators, each of which is a product of a parameter and its associated coefficient operator where the operator is the theoretical factor and where the parameter must be obtained either from experiment or from the use of the AOC-DFT computational model.

The concept of orthogonality derives from the idea of a scalar product (or overlap) [19,53] of a pair of operators $\hat{A}$ and $\hat{B}$, which for real matrices is defined by

$$\langle \hat{A}|\hat{B}\rangle = \sum_{i,j} \mathbf{A}_{ij}\mathbf{B}_{ij} \quad (1)$$

The value of this operator overlap is independent of the function basis in which the matrices are set up. The fact that only energy differences are observable as empirical parameters of ligand-field theory is often built into the model by barycentration, in which case the weighted sum of the energies of the complete set of d^q states is made equal to zero [20]. Thereafter, the sum of the (barycentered) energies is equal to zero and the root mean square splitting may be taken as a measure of the average energy splitting of the (barycentered) d^q configuration. The degeneracy-weighted sum of the squares of the eigenenergies of all the states is referred to as the sum square splitting (SSS) of the configuration. The SSS is related to the overlap of Eq. (1) by being the self-overlap of the barycentered Hamiltonian. For any fitted model describing the experiment, the modeled sum-square splitting obeys an energy-inverted variational principle and will always be lower than the experimental one (or DFT-computed one) [20]. Furthermore, if the model is a sum of mutually orthogonal operators, the sum square splitting is a sum of contributions from the individual parameters: that is, it does not contain cross products of parameters.

In its general formulation, the orthogonal operator's method focuses on operator overlaps defined over the entire d^q space including non-diagonal contributions. A special situation arises when the function basis is fixed and only the diagonal part of the operator overlaps is considered. This situation is encountered when the DFT energies associated with the Slater determinants are equated with the parameterized energies of the appropriate strong-field LF. This special situation is enforced by the nature of the DFT method where only the Slater determinantal diagonal contributions to the *R* part of the LFR Hamiltonian can be accessed [13]. The result is that operator orthogonality and parameter independence become synonymous [4]. Thus, the mimicking process revives the orthogonal operator's method and provides an invitation to use a symmetry-based partitioning of LF as well as *R*. We shall not review the use of the orthogonal operator's method further here but refer to the repeated use of it throughout Sections 3 and 4.

The actual process of mimicking LFR by DFT consists of a series of discrete steps. These have been discussed at length and illustrated by concrete examples in previous applications of the method [4,21,22]. Characteristic of the method is that it involves two SCF computations. The first one is an unrestricted computation whose primary purpose is an optimization of the geometry that is to be used for all the following ligand-field mimicking. This computation may also be used to identify the unrestricted eigenorbitals of the system in question. The second SCF computation provides the connection with LFR and in the first place only with the LF part of LFR. This computation is not only spin-restricted, but also constrained by having a starting point where the ten d spin-orbitals share the *q* electrons of d^q equally. The SCF result of this computation is that the molecular "d" orbitals keep this sharing property and that the associated AOC density is totally symmetric in the point group of the molecular system and is spherical if the system is atomic in character. The main purpose of this restricted Kohn-Sham computation is the acquisition of the eigenorbitals of this AOC state and their KS orbital energies. These eigenorbitals make the basis for building up the Slater determinants whose energies are to be computed in all the following non-SCF computations where these eigenorbitals remain unchanged (frozen). For the problem of mimicking the LF alone, it is important that the molecular "d" orbitals can be mapped individually upon the LF d orbitals. For the mimicking of LFR, we use the corresponding individual mapping of the KS Slater determinants upon LFR Slater determinants. The resulting equations relating DFT energies and LFR parameterized expressions for the energies of the Slater determinants are solved by the least squares method to obtain the values for the LFT parameters, which should be directly comparable with the empirical parameters of the Parametrical d^q Model.

3. Results for axially compressed systems with one strong-donor ligand

The coordination chemistry of multiply bonded ligands such as oxide, nitride, imide and carbide has gained renewed interest in recent years due to their importance in processes involving the activation of small molecules in biological systems as well as in industrial catalysis. These ligands present special challenges in the context of ligand-field descriptions since the spectroscopical information is limited by the nature of the ligands. Thus, a frequent situation is that the systems stabilized by these strong donor ligands are d^0 systems or that the spectroscopy is dominated by electron-transfer transitions (LMCT) [10b], which prevents experimental determination of the metal d-orbital energies and thereby the comparison between theory and experiment. In addition, the σ-perturbation from strongly donating ligands is in almost all cases of such a magnitude that direct determination by optical spectroscopy is ruled out by the high energy of the excited state and the best one can hope for is to determine the associated parameter(s) by indirect ways or by computational methods. The computation of σ-perturbation parameters for such systems is, however, not entirely without connection with experiment: the σ-perturbation will in some cases influence ground-state properties such as zero field splittings, *g*-values or Mössbauer parameters, and the magnitude of the σ parameter can thereby with some uncertainty be estimated from experimental data. It follows from the above comments that the optimal auxiliary ligand systems to a strong-donor-ligand system, as far as bridging between ligand-field theory and experiments is concerned, are systems with as small ligand-field splittings as possible and involving simultaneously spectroscopically innocent ligands, thus leaving as much of the d–d spectral range as possible uncovered by electron-transfer and internal-ligand transitions.

3.1. Strong-donor systems with observable d–d transitions

The requirement for weak auxiliary ligand fields makes complexes of the first-row transition metals the systems of choice. However, unlike the situation for other ligands, the chemistry of the first-row transition elements is much less developed than that of the second- and third-row transition metals for the strongly donating ligands. This is particularly true for the nitrido ligand (N^{3-}), which is the strongest donor for which spectroscopic information is available and thus the most interesting one. Until a decade ago the nitrido complexes that were known with spectroscopically transparent ligands were limited to complexes of the second- and third-row transition metals.

The nitrido chemistry of the first row transition metals was confined to a handful of systems, the first of which, Cr(N)(salen), was reported by Ashankow and Poznjak in 1981 [23]. In 1983 Buchler et al. reported the first synthesis of nitridomanganese(V) complexes. These were with porphyrins as auxiliary ligands [24] and several years later the corresponding nitridophthalocyaninatomanganese(V) species were synthesized [25]. The first non-porphyrin manganese nitrido complex, Mn(N)(salen), was reported by Carreira and coworkers in 1996 [26] and

the same year the first octahedral manganese nitrido complex, $[Mn(N)(acac)(tmtacn)]^+$, was reported by Wieghardt and coworkers as the first nitride complex for which d–d transitions could be observed [27]. Shortly thereafter truly spectroscopically rewarding systems encompassing $[M(N)(cyclam)(CH_3CN)]^{2+}$ [28,29], $[M(N)(CN)_5]^{3-}$ [30], $[M(N)(CN)_4]^{2-}$ (M = Cr, Mn) [31], and more recently $[Cr(N)X_4]^{2-}$ (X = NCS, N_3) [32] and the simplest one, $[Cr(N)Cl_4]^{2-}$ [33], were synthesized and spectroscopically characterized.

While different authors have studied many aspects of nitride coordination chemistry by DFT, including super-hyperfine couplings and nitride activation reactions, our application of DFT to nitrido complexes has focused on a more narrow range of objectives, where our main contributions concern electronic structure investigation in the ligand-field regime.

3.2. The ligand-field description of electronically, strongly compressed systems

The point of departure for a ligand-field analysis of the nitrido complexes in question is the orbital energy splitting diagram shown in Fig. 1. The diagram assumes a tetragonal ligand field with a strong donor ligand on the *z*-axis.

For the d^1 systems a suitable LF parameterization of these splittings is the only prerequisite. We emphasize here that qualitatively different splittings with different energetic ordering of the $d_{x^2-y^2}$ orbital and the $\{d_{xz}, d_{yz}\}$ set of orbitals are found experimentally and reproduced by DFT calculations for oxide or nitride as the strong donor-ligand [32]. For d^2 systems, there exists the possibility of two different ground states. For a small to moderate perturbation of the octahedral reference situation, with a resulting moderate splitting of the octahedral t_{2g} set of orbitals, the ground state is expected to be a spin triplet. However, for very strong π-donor ligands, the resulting large splittings of the t_{2g} set of orbitals will favour spin pairing and a singlet ground state. When the orbital energies of such an electronically anisotropic tetragonal system (D_{4h} symmetry by holohedrization) are parameterized by the angular overlap model (AOM) and combined with the conventional spherically based parameterization of the interelectronic repulsion, the sequence of complete energy level diagrams encompassing all the states of the d^2 configuration in tetragonal symmetry, can be derived (cf. Fig. 2). The first figure shows the cubic strong-field configurations, separated into multiplets by the interelectronic repulsion interaction. The second and third figures are concerned with the tetragonal anisotropies caused by different perturbation contributions from the axial and equatorial ligands. The primary points to make from these diagrams is that it is the anisotropy in the AOM π-parameters, which causes the change in spin of the ground state. Moreover, a numerically high value for this π-anisotropy is required to reach the low-spin situation. The experimental fact that d^2 systems with multiple-bonded ligands almost exclusively are low-spin (see Ref. [34] for a possible exception) then puts a lower limit on the possible values for the AOM π-parameters of the strongly donating ligands. This limit is of course formally correlated to the values of the interelectronic repulsion and the π-parameter values for the equatorial ligands. It remains, however, that a simple consideration of the type in Fig. 2 in combination with our knowledge of approximate values for the interelectronic parameters, provides an important boundary condition on the π-parameters of oxide and nitride ligands showing that these parameters must be large enough to match σ-parameter values of weak donors. The transferability assumption sometimes associated with the AOM makes this result extendable to chemically related d^1 systems, wherein we also expect e_π parameter values above 10,000 cm^{-1} and therefore a $d_{xy} \rightarrow d_{x^2-y^2}$ transition observable in the visible or NIR range.

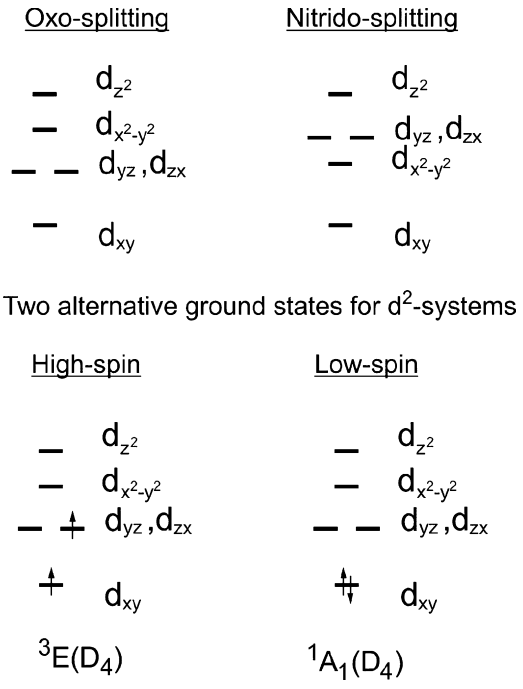

Fig. 1. *Top*: d-orbital splitting diagrams for mono-oxo and nitrido complexes. *Bottom*: alternative spin ground states for d^2 systems with strong donor ligands.

For the d^1 as well as the d^2 systems, the descriptions based on the AOM are actually overparameterized, but that problem was partly overcome in the LFT analysis by chemically based assumptions (no π-interaction for saturated amines (cyclam) and linear ligation for cyanide and acetonitrile ligands). It remained, however, that only one repulsion parameter was determined for the d^2 cases [28].

When comparing DFT calculations on these systems with the ligand-field description, we found in general a good correspondence, but one result stood out and clearly demonstrated the limitations at least of conventional ligand-field models. In the diagrams shown in Figs. 1 and 2, the systems are parameterized in their holohedrized geometries, since the parity of the d-orbitals has the consequence that only the sum of the parameters attributed to *trans*-situated ligands enters the ligand-field expressions. While this is the best one can do in an additive model, it is obvious that it results in rather different descriptions for the five and six-coordinate complexes. In the latter systems, ligand-field descriptions, which by convention are restricted to the d-orbital space, only allow the determination of the sum of the ligand-field parameters of the nitride ligand and the *trans*-situated ligand. This would appear to be a minor complication since a range of five coordinate systems are known from which the "pure" parameters of the nitride ligand can be determined, and by assuming the parameter transferability normally invoked in the AOM, this allows partitioning of the parameter sums determined from the six-coordinate systems. Furthermore, the contribution from the ligand situated trans to the nitride would be expected to be small due to the very large influence of the nitride ligand upon the distance of this *trans*-ligand from the metal (cf. Table 1) and thereby upon the ligand-field contributions from this *trans*-ligand.

Assuming the ligand-field parameters to vary with r^{-5} would, everything else apart, make the *trans*-ligand contribution to the axial ligand field less than 10%. These considerations indicate that from a quantitative point of view, the ligand-field description of the five- and six-coordinate complexes should be quite similar. However, in this respect the LFT and DFT descriptions diverge due to a qualitative difference.

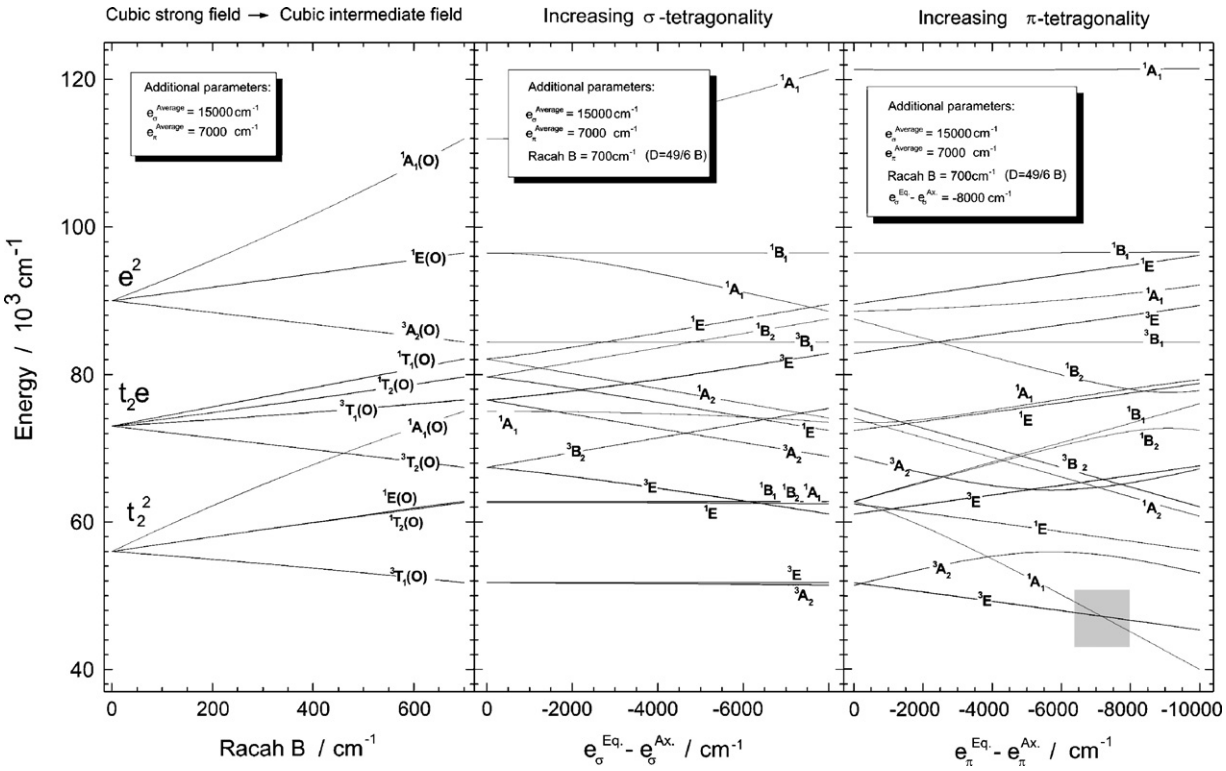

Fig. 2. A three-step energy level diagram for the d^2 configuration. The ligand field of the generic *trans*-$ML^{Ax.}{}_2L^{Eq.}{}_4$ is parametrized with one π-parameter per ligand type (linearly ligating ligands). The shaded box is the high-spin/low-spin crossover. The right-most part of the diagram shows that a pronounced π-anisotropy is required in order to reach the spin crossover to low-spin d^2 systems (shaded area).

The DFT results for $[Cr(N)(CN)_4]^{2-}$ showed the function with the largest $3d_{z^2}$-content (Fig. 3) to be a strongly mixed $3d_{z^2}$-$4p_z$ (also with a significant 4 s content [42]) orbital, thus a function not belonging to the ligand-field basis. This orbital becomes less antibonding, that is, it obtains a lower energy in the DFT description by becoming polar in such a way that it is partially directed away from the nitride ligand. The alternative assignments for the first excited state in the five coordinate cyano complexes, with the e (normal ligand-field picture) respectively the a_1 ($3d_{z^2}/4p_z$ mixing) populated were evaluated. The conclusion was that both assignments could explain the observed vibrational fine structure in the absorption spectra and that in the absence of polarized spectra, which were only available for six-coordinate species, it was impossible to rule in favour of either assignment [30].

This situation illustrates nicely the advantage of combining LFT and DFT modeling: without the ligand-field analysis, the unique nature of the bonding situation introduced by the very strong ungerade component of the ligand field would not be noticed. For a LF model, even if extended with central-ion d–p mixing caused by the ungerade (hemihedric) part of the ligand field, no stabilization would occur from a mixing of the two empty orbitals. An MO description, on the other hand, recognizes the possible stabilizing effect on the binding, populated and mainly ligand character orbitals arising from d–p mixing. Since the orbital depicted in Fig. 3 is empty in the ground state it is not very well defined in the variational DFT approach. Its shape and composition does, however, not vary discontinuously when it is slightly fractionally populated. Such *l*-mixing has been discussed in several contexts during the development of LFT [43a–c, 43e–g] and recently, similar d–p hybridization has been observed in DFT calculations on imido complexes in other geometries [43d]. The novel situation is that DFT allows an easy

Table 1
Bond lengths demonstrating the *trans* influence in some complexes of strong π-donor ligands (oxide/nitride) and a carbyne complex.

Complex	$d_{M\text{-}L(trans)}$ (Å)	$d_{M\text{-}L(cis)}$ (Å)	$d_{M\equiv X}$ (Å)	Reference
$[V(O)(H_2O)_5]^{2+}$	2.4	2.1	1.591(5)	[35]
$[Nb(O)Cl_5]^{2-}$	2.555(4)	2.40(2)	1.967(6)	[36]
$[Os(N)Cl_5]^{2-}$	2.605(4)	2.362(5)	1.614(13)	[37]
$[Cr(\equiv CNEt_2)(CO)_5]^{+}$	1.98	1.87	1.797(9)	[38]
$[Mo(O)(CN)_5]^{3-}$	2.373(6)	2.178(6)	1.705(4)	[39]
$[Re(N)(NCS)_5]^{-}$	2.301	2.02	1.657(12)	[40]
$[Os(N)(CN)_5]^{2-}$	2.353(8)	2.08(2)	1.647(5)	[41]
$[Cr(N)(CN)_5]^{2-}$	2.060(14)	2.299(12)	1.594(9)	[30]
$[Mn(N)(CN)_5]^{2-}$	1.990(7)	2.243(7)	1.499(8)	[30]
$[Cr(N)(NCS)_3(phen)]^{2-}$	2.0973(19)	2.321(2)	1.563(2)	[32]

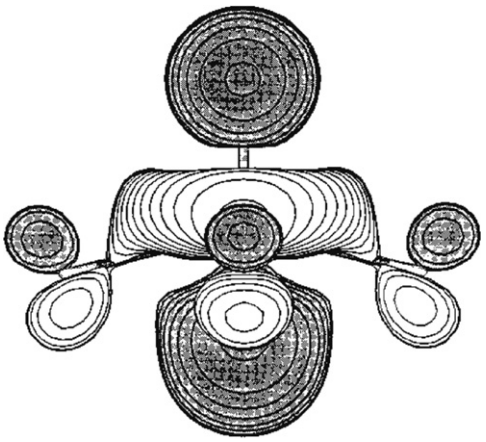

Fig. 3. The orbital with the largest $3d_{z^2}$-content for $[Cr(N)(CN)_4]^{2-}$, exhibiting pronounced d–p mixing.

Table 2
Calculated Mulliken charge distribution in chromium(V) nitride complexes.

	$[Cr(N)F_4]^{2-}$	$[Cr(N)Cl_4]^{2-}$	$[Cr(N)Br_4]^{2-}$	$[Cr(N)I_4]^{2-}$
Charge (Cr)	1.29	0.70	0.88	0.35
Charge (N)	−0.56	−0.35	−0.33	−0.28
Charge (X)	−0.68	−0.59	−0.64	−0.52

quantification of the purity of d^q configurations. We have also observed it in regular tetrahedral complexes [22].

It is in this context worth to note that the relationship between the strong axial compression found in (low-spin) d^2 systems and the strong axial elongation in (low-spin) d^8 systems extends beyond the geometrical complementarity, which we have pointed to earlier [3a]. Not only do these electronic configurations, which are connected by the hole-electron correspondence, distort in complementary ways, they are also connected by their propensity to mix in functions with different *l*-values into the metal d-orbitals. The two configurations show complementarity also with respect to their tendency to *l*-value mixing since the five-coordinate d^2 systems feature the strong *ungerade* component of the ligand field, while the d^8 systems have inversion symmetry.

The low-spin d^2 electron configuration $(d_{xy})^2$ can, however, also be obtained for systems with an inversion-symmetric ligand field, but only if the strong donor ligands are oxo-ligands, as exemplified by the complexes *trans*-$M(O)_2(dppe)_2$ (M = Mo,W), *trans*-$[Re(O)_2(py)_4]^+$, and *trans*-$[Os(O)_2(OH)_4]^{2-}$ [44a,44b]. Here we have an illustration of the qualitative difference in donor strength of nitride and oxide ligands. Nitride is such a strong donor that no examples are known wherein more than one nitride ligand is coordinated to the same metal centre – the strongest donor found trans to a nitride ligand is hydroxide in the system *trans*-$[Os(N)(OH)(CN)_4]^{2-}$ [44c]. The strong donation from the nitride ligand is also manifest in the reactivity of nitride complexes and in the DFT-calculated charge distributions which correlate well with the experimentally observed variation of nucleophilicity of nitride complexes [30,45].

Several authors have noted the strong covalency in the M≡N bonds and the concomitant charge levelling in these complexes. For the series of halide complexes $[Cr(N)X_4]^{2-}$ (X = F, Cl, Br, I) the calculated Mulliken charges on Cr and N are comparable to those found on the metal and ligands of classical Werner-type chromium(III) complexes [33] (Table 2). This is in line with a combined experimental and DFT study which found that for a wide range of spectroscopically characterized Cr(V)–nitride systems, the spectrochemical series of the auxiliary ligands was not only parallel to that derived from Werner-type coordination complexes, but it was numerically almost coincident with that series [32]. The charge levelling is also consistent with the insensitivity of the DFT calculated electronic structure towards solvation modeling. There is, however, a pronounced dependence of the charges within the $\{Cr(N)\}^{2+}$ moiety on the remaining coordination sphere cf. Table 2), which might have as a consequence that the transferability of parameters, which often is assumed in additive ligand-field parameterizations, holds less well for this class of complexes. However, the unsystematic order of metal charges in the chloride and bromide complexes parallels the situation found for tetrahedral halide complexes (cf. Table 7) and if it is assumed that a closer comparison of Tables 2 and 7 is allowed, it may be concluded that the moiety corresponds to a central ion with an oxidation state slightly smaller than three with regard to its polarising properties of halide ligands. The small charge separation and strongly covalent nature of the M–N triple bond has also been discussed in the context of a comparison between nitride and nitrosyl complexes [46].

3.3. On the reference geometry for $[Cr(N)X_4]^{2-}$ – a distorted linear or a distorted octahedral system?

Our discussion and understanding of coordination chemistry is intimately connected to reference geometries of high symmetry and an implicit hierarchical symmetry analysis. Irrespective of whether molecular or electronic structure is discussed, we describe real molecules with reference to idealized structures or energetic splitting patterns. In a few cases the intuitive choice of reference symmetry is more misleading than guiding. The nitride complexes with weak auxiliary ligands constitute such an example. The Mn–N distance, for example, can be as low as 1.50 Å to be compared with the normal bond lengths of ca. 2 Å (Table 1). The short bond lengths accompany very special donor properties of the nitride ligand resulting in a partial break-down of the link between molecular and electronic structure: since some of the five-coordinate Cr-nitride complexes can take up an extra ligand and thereby become six-coordinate, geometrically distorted octahedral systems, it is natural to consider the five-coordinate square-pyramidal systems as derived from the octahedron. However, based on the energetic ordering of the d-orbitals as determined spectroscopically and corroborated by DFT calculations, linear symmetry appears as the more natural reference symmetry. In the linear symmetry, which is used as a basis for additive LFT, the energy is a function only of $\lambda = |m_l|$ with the ordering $e(\delta) < e(\pi) < e(\sigma)$. The fact that both δ-orbitals (d_{xy}, $d_{x^2-y^2}$), although not degenerate, are lower in energy than the π-set of orbitals (d_{yz}, d_{zx}) and the d_{z^2} (irrespective of its lack of purity) is higher in energy (and experimentally unobserved in $[Cr(N)Cl_4]^{2-}$), forms the simple basis for its classification as a perturbed linear system. A more rigorous and quantitative method of comparing the individual parts of the ligand field was introduced into ligand-field theory in the context of the orthonormal operators formalism [19]. In this description it is possible to partition the total squared energetic splitting of the d^q configuration into independent contributions from each term of the ligand-field Hamiltonian, provided these terms are described by mutually orthogonal operators. This requirement is met when the ligand field is parameterized in a symmetry hierarchy, e.g. $O_h \supset D_4 \supset D_2$. However, the requirement is not met for a description in terms of symmetries, which do not have the supergroup–subgroup relationship. Therefore, it is not possible to make a quantitative partition into octahedral and linear contributions of the sum square splitting (SSS) of the d-function space of $[Cr(N)Cl_4]^{2-}$. We may, however, parameterize the ligand field in either of the hierarchies $O_h \supset C_{4v}$ and $C_{\infty v} \supset C_{4v}$ and within each of these parameterizations obtain a rigorous quantification of the relative importance of the high- and low-symmetry terms. In order to make such an analysis feasible, we need to know the energies of the complete set of d-orbitals including the high-lying and experimentally unobserved d_{z^2}. Here DFT calculations come to the rescue by providing the required complete set of orbital energies, which for the purpose of mapping onto the LFT description, are most consistently obtained by an AOC calculation. The analysis when based on the eigenfunctions obtained directly from the DFT calculation will of course include explicitly the covalency and it will therefore lack some of the function basis invariance and thereby some of the beauty from the original formulation in the LFT framework. It should also be stressed that the significant mixing of 4p and 4s into $3d_{z^2}$ affects the rigor of the analysis and we neglect that difference in function bases in the process of projecting the DFT results onto LFT.

In addition to furnishing the necessary energy information for the full d-space, DFT allows a direct bridge between geometrical and electronic structure to which LFT does not directly lend itself: by letting the geometry of the system in question be an independent parameter and calculating the d-orbital energies for different

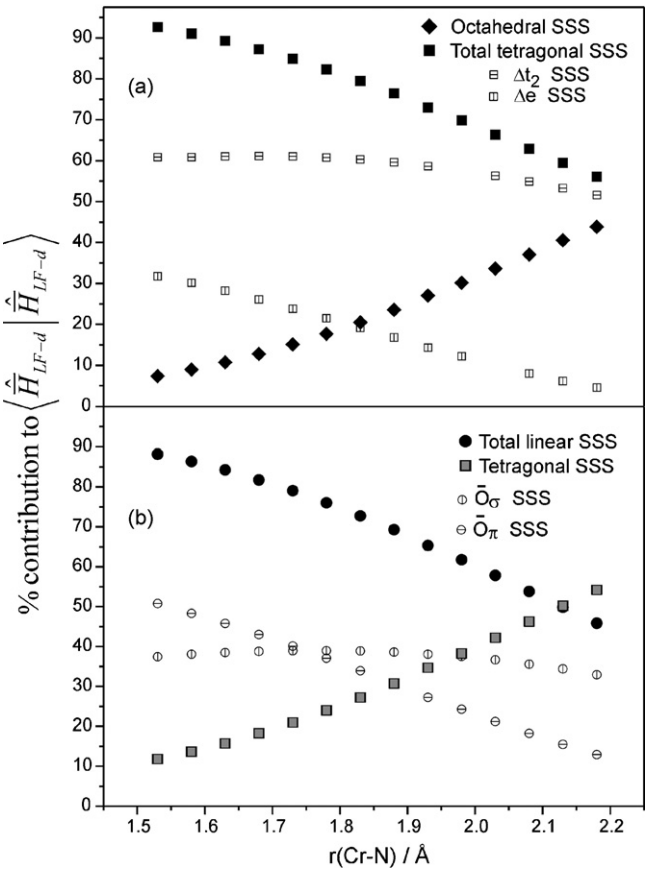

Fig. 4. Relative contributions to the sum square splitting of the d-space of $[Cr(N)Cl_4]^{2-}$, when parameterized in the two hierarchies $O_h \supset C_{4v}$ (a) and $C_{\infty v} \supset C_{4v}$ (b). The filled markers represent the uniquely defined partition into symmetry contributions octahedral/tetragonal and linear/tetragonal. The open markers represent the subdivision of respectively the tetragonal and linear ligand fields in the two hierarchies. cf. Fig. 5 for the definition of the individual parameters.

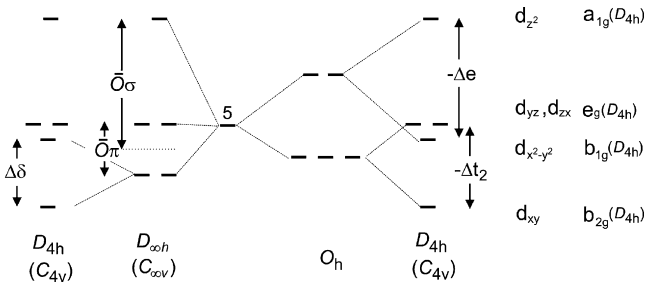

Fig. 5. Definition of the symmetry-derived ligand-field parameterization in the two hierarchies $O_h \supset D_{4h}$ ($O_h \supset C_{4v}$; right) and $D_{\infty h} \supset D_{4h}$ ($C_{\infty v} \supset C_{4v}$; left). The group labels in parentheses are the actual molecular symmetries, while those without are the holohedrized symmetries imposed by making the correspondence with LFT. The parametrization in the latter hierarchy has been chosen to reflect chemical intuition for a linear system: the first parameter, O_σ, separates the σ orbital from the rest while maintaining the barycentre. The second parameter, O_π, separates the π-set of orbitals from the δ-set, again with conservation of the barycentre. Finally, the last parameter $\Delta\delta$, which is of tetragonal symmetry and proportional to the corresponding parameter of the crystal-field parameterization [49], describes the separation of the two δ-orbitals, d_{xy} and $d_{x^2-y^2}$. Orthogonality of the associated operators is secured by the barycentration of all three splittings.

geometries, it is possible to relate directly the electronic structure quantified by the orthonormal operators method to geometrical variables (distortions). We illustrate these two virtues of DFT in Fig. 4 where the outlined methodology [6] has been applied to $[Cr(N)Cl_4]^{2-}$.

For the system in its experimental geometry (r(Cr–N) = 1.559 Å) we find that the ligand field is ca. 10% octahedral and 90% tetragonal in the $O_h \supset D_{4h}$ ($O_h \supset C_{4v}$) hierarchy. Conversely, we find the system to be 90% linear and 10% tetragonal in the $D_{\infty h} \supset D_{4h}$ ($C_{\infty v} \supset C_{4v}$) hierarchy. However, thereby the whole concept of a hierarchical parameterization of the ligand field becomes meaningless in the former description, where the high-symmetry contribution amounts to only ca. 10% of the total perturbation of the configuration. Although it is for fundamental reasons not possible to simultaneously quantify the octahedral and linear contributions to the splitting of the ligand-field function space, it is clear from the above analysis that a hierarchical, symmetry-based parameterization of the ligand field only is conceptually coherent when done in the linear hierarchy.

Furthermore, the situation is for this system so clear-cut that in the most natural, although not unique, sub-parameterization of the tetragonal field in the $O_h \supset D_{4h}$ ($O_h \supset C_{4v}$) hierarchy, the octahedral contribution to the SSS remains smaller than that from either of the independent tetragonal parameters (Δe and Δt_2) and in the $D_{\infty h} \supset D_{4h}$ ($C_\infty \supset C_{4v}$) parameterization, the tetragonal contribution ($\Delta\delta$) is smaller than that from either of the independent linear ligand-field parameters (O_σ and O_π). From the variation of the contributions to the total SSS with Cr–N bond length, it is seen that there is an almost linear variation of the relative importance of the linear ligand field with Cr–N bond length in the range 1.53–2.00 Å where the $C_{\infty v}$ contribution to the SSS decreases from ca. 88% to ca. 59%. This variation underestimates the difference between actual chemical systems since the analysis is based on variation of only the Cr–N bond length without simultaneous optimization of the remaining coordination sphere, the importance of which is expected to increase also in absolute terms as the strongly donating nitride ligand is moved away.

It should also be noted from Fig. 4 that at the experimental M–N bond lengths (M = Cr, Mn) the π-contribution to the total SSS exceeds the σ-contribution, which gives a coherent picture when taken together with the low-spin ground state of the d^2-systems and Fig. 2. Moreover, from MO energetics of diatomic molecules it is known that π bonding becomes especially important at short bond distances.

3.4. Additive ligand-field parameterizations: avoiding over-parameterization by extension of the DFT-LFT mapping with vibronic coupling expressions (DFT-LFT-VC)

The above discussion was conducted in a symmetry-based (holistic) ligand-field parameterization scheme, which has the advantage of encompassing exactly the number of independent parameters allowed for by symmetry. In our example we saw an exact parameterization of the three orbital energy differences. The symmetry partition, as performed above, is rigorous and the problem of over-parameterization frequently encountered in LFT modeling is not present in our previous example. We can apply DFT to the complete series of nitride–halide complexes of Cr(V): $[Cr(N)X_4]^{2-}$ (X = F, Cl, Br, I) and obtain the level splitting diagram of Figs. 1 and 5. As above, a set of symmetry-based ligand-field parameter values could be extracted for each system. However, the potential of LFT for systematizing coordination chemistry is better unleashed in the chemically inspired additive parameterization scheme of the angular overlap model. Considering the system $[Cr(N)Cl_4]^{2-}$, an additive parameterization of the ligand field encompasses in the AOM four parameters e_σ^N, e_π^N, e_σ^{Cl}, e_π^{Cl}, which cannot all be extracted neither from a hypothetical experiment where all the d-levels were observed nor from a DFT calculation of the d-subspace energies.

However, a barycentered AOM parameterization of the four levels, based on the DFT-optimized geometry of the complex, with the

DFT-calculated energies, yields a linear equation system of rank three, reflecting that the barycentre is external to the ligand-field model and that only three independent pieces of data are available. The situation is exemplified for an AOC-DFT/AOM modeling of $[Cr(N)Cl_4]^{2-}$, which is condensed in the equation system shown below where the right-hand side consists of AOC-DFT data while the left-hand side is the purely mathematical consequence of the AOM parameterization of the DFT optimized geometry:

$$\begin{aligned}
\bar{E}(d_{xy}) &= \bar{E}(\delta s) = -0.2\,e_\sigma^N - 0.4\,e_\pi^N - 0.8\,e_\sigma^X + 2.17273\,e_\pi^{Cl} = -2.004\,\text{eV}\\
\bar{E}(d_{x^2-y^2}) &= \bar{E}(\delta c) = -0.2\,e_\sigma^N - 0.4\,e_\pi^N + 1.86878\,e_\sigma^X - 1.386554\,e_\pi^{Cl} = -0.668\,\text{eV}\\
\bar{E}(d_{xz}, d_{xz}) &= \bar{E}(\pi s, \pi c) = -0.2\,e_\sigma^N + 0.6\,e_\pi^N - 0.478465\,e_\sigma^X + 0.0849215\,e_\pi^{Cl} = 0.592\,\text{eV}\\
\bar{E}(d_{z^2}) &= \bar{E}(\sigma) = 0.8\,e_\sigma^N - 0.4\,e_\pi^N - 0.11185\,e_\sigma^X - 0.95693\,e_\pi^{Cl} = 1.487\,\text{eV}
\end{aligned} \tag{2}$$

The nullspace of the equation system has dimension one and is spanned by the vector:

$$\vec{n} = \{0.685166\,e_\sigma^N, 0.513873\,e_\pi^N, 0.412975\,e_\sigma^{Cl}, 0.309732\,e_\pi^{Cl}\}$$

In other words: all four parameters cannot be determined unambiguously – to any solution, an arbitrary scaled nullspace vector can be added and it will remain a solution. It would appear that the problem is as unavoidable as it has been throughout the development of additively parameterized ligand fields. However, the AOM very conveniently handles angular distortions without introducing additional parameters. We can thus parameterize the angular variation of the energies of the d-levels for small distortions around the DFT-optimized geometry using the AOM and by applying DFT in parallel obtain values for the energies thus parameterized. By this extension of the DFT/LFT mapping to encompass also the linear vibronic coupling coefficients, we obtain additional linearly independent equations in the AOM parameters. The number of additional equations will equal the number of components of normal vibrations minus the number of ligands (for monatomic ligands) although these equations are not all guaranteed to be linearly independent. Consequently, systems which in a conventional treatment are overparameterized will in general become over-determined by full application of this approach [21]. This idea builds on the early insight of Bacci that vibronic coupling coefficients for angular distortions can be analytically calculated within the framework of the AOM [47a–c]. The approach has also been used in a couple of other specific applications to obtain values for otherwise undetermined parameters [47d,e].

The merging of vibronic coupling parameters and AOM parameters provides either for direct calculation of vibronic coupling strengths using no further assumptions or it allows for vibronic coupling data to function as additional and independent observables for furnishing AOM parameters. It is with the latter focus that DFT combined with AOM-parameterized vibronic coupling maximizes the information extracted from DFT and projected on LFT. We conclude our discussion of this method by the simplest possible application to the tetragonally perturbed linear chromium nitrido complexes. Let us supplement the AOM expressions for the d-orbital energies with an expression for the totally symmetrical umbrella vibration distorting the N–Cr–X angle. When the AOM expressions are set up and linearized around the DFT-optimized geometry ($\theta = 103.79^\circ$), we obtain the following expressions for the d-orbital energy dependences on the distortion angle (α):

$$\begin{aligned}
\frac{\partial(E(\sigma) - E(\delta s))}{\partial\alpha} &= -2.30442\,e_\sigma^{Cl} + 6.77645\,e_\pi^{Cl}\\
\frac{\partial(E(\pi s, \pi c) - E(\delta s))}{\partial\alpha} &= 2.46225\,e_\sigma^{Cl} - 0.505082\,e_\pi^{Cl}\\
\frac{\partial(E(\delta c) - E(\delta s))}{\partial\alpha} &= -2.62009\,e_\sigma^{Cl} + 3.49345\,e_\pi^{Cl}
\end{aligned} \tag{3}$$

Table 3
Angular overlap model parameters (cm^{-1}) extracted from a combination of energy expressions and linear vibronic coupling coefficients equated to DFT results.

	$[Cr(N)F_4]^{2-}$	$[Cr(N)Cl_4]^{2-}$	$[Cr(N)Br_4]^{2-}$	$[Cr(N)I_4]^{2-}$
e_σ^N	27,530	29,800	24,200	22,900
e_π^N	17,720	22,960	19,760	20,690
e_σ^X	7,720	6,700	3,150	3,430
e_π^X	1,540	1,990	−290	0

It is easy to verify by inspection that this set of equations has two independent equations and when the expressions for the orbital energies are combined with these equations a set of equations of rank 4 is obtained. The same is true if the orbital energies are supplemented with either of the first two vibronic coupling equations, but not if the third, which is linearly dependent on the orbital energy expressions, is employed. For idealized geometries some linear vibronic coupling coefficients vanish for symmetry reasons. This is, for example, the case for all the expressions above in the idealized square pyramidal geometry ($\theta = 90^\circ$) and in such cases either the expressions have to include quadratic terms or preferably other geometric distortions used as the sources for the parametric restraints. The numerical values of the left-hand sides of the vibronic coupling equations are obtained from two AOC-DFT calculations. By substituting the first of the resulting vibronic coupling equations for the last of the orbital energy expressions of Eq. (2) and solving the resulting four equations, the following parameter values are obtained $e_\sigma^N = 29,800\,cm^{-1}$, $e_\pi^N = 22,960\,cm^{-1}$, $e_\sigma^{Cl} = 6700\,cm^{-1}$, $e_\pi^{Cl} = 1990\,cm^{-1}$. AOM parametric results obtained in this way for all four $[Cr(N)X_4]^{2-}$ (X = F, Cl, Br, I) complexes are collected together in Table 3. They illustrate the strength of the present methods in terms of quantification of chemical variation. As with the variation in charge distributions, an irregular variation between chloride and bromide is observed. We emphasize that the situation selected here is among the least favourable ones possible because the vibration employed here does not lower the symmetry and thereby does not introduce new energy splittings.

In the next chapter we discuss ligand-field parameters for homoleptic tetrahedral complexes and in this context how the DFT-LFT-VC approach described above has been used to extract σ-, as well as π-AOM parameters for halide ligands.

4. Quantitative ligand-field theory: results for tetrahedral complexes

In order to illuminate the LFR model by DFT, we have treated eight d^2 tetrahedral molecular systems with V^{III} and Cr^{IV} as representative central ions and with halide ions as representative ligands. These complexes have $^3A_2(T_d)$ ground states and are therefore in the LFR model independent of Jahn–Teller distortion problems. A discussion of the LFR model and its relationship to DFT is therefore particularly relevant for these chemical systems.

4.1. Density functional theory partnering ligand-field theory: the ligand field and the interelectronic repulsion

When the molecular symmetry is T_d, holistic or non-additive LF theory [3,48], which is based solely on the mathematical theory of groups, tells us that the d orbitals fall in two energy classes

belonging to the symmetry species (irreducible representations) $e(T_d)$ and $t_2(T_d)$, and these two symmetry species can likewise be found in the AOC-DFT results. Within LFR, empiricism tells that the t_2 class has the higher energy and as our first qualitative results, the same is found in AOC-DFT for all our eight complexes. We shall soon see that this qualitative empirical result, which was universally adopted 50 years ago, can be rationalized by combining the relative positions of the ligands with the linear symmetry of the M-L sub-systems (additive LF).

Already at the orbital energy level, there is a one-to-one relationship between LFR and AOC-KS-DFT, and the primary practical consequence is that the latter provides the radial one-electron parameters of the former and thereby quantifies the relationship between the two independent and fundamentally different models: the atomic LFR and the molecular KS-DFT.

The completely additive LF is defined [49,50] by the condition that barycentered LF-contributions from all the individual ligands add up to the total barycentered LF, equalized to the holistic LF. Thereby, two completely different parametric descriptions of the same ligand field are obtained [21]. The parameterization of the angular overlap model refers to the symmetry species of the point group $C_{\infty v}$ of the M-L sub-systems when L is monatomic [51,52]. These are σ and π, simultaneously referring to the individual ligand to metal bonds, and the parameters e_σ and e_π conventionally refer to the additive model that was used in Section 3.

The σ orbitals of the four ligands fall in classes characterized by symmetry species of T_d, namely a_1 and t_2. This statement is independent of whether the σ orbitals of the ligating atoms originate in s, p, or d orbitals of this atom. Moreover, with reference to the vibronic discussion of Section 3.4, the same statement applies to the stretching vibrations of the four metal-ligating atoms contacts. The angular overlap model focuses upon the t_2 orbitals and sees a possible bonding interaction: the dt_2 orbitals of the central ion and those of the ligating ions may σ-interact under the Hamiltonian of T_d symmetry, and since it is known experimentally as well as from AOC-DFT that the filled t_2 orbitals classified as ligand orbitals have the lower energy, the dt_2 orbitals of the central ion have become the antibonding partners. Therefore, the AOM with its primary focus on the energy-dominating σ interactions [68] immediately provides the qualitative statement that the dt_2 orbitals have the higher energy of the two d-orbital classes, de and dt_2, in T_d.

With its molecular orbital view, the AOM parameterizes the energy of the dt_2 orbitals as $(4/3)e_\sigma$ as can be found by using its sum rule for coefficients to the MO parameters of the AOM, which in this case runs as follows: the sum of the coefficients to the e_σ parameters of the three t_2 orbitals is equal to the number of ligating atoms.

With the ligand-field view of the AOM [49,50], the energies of the e and the t_2 orbitals have to be barycentered, that is, their average energy according to the sum rule for coefficients, $(4/5)e_\sigma$, has to be subtracted so that the energies of e and t_2 orbitals become $-4/5$ and $((4/3)–(4/5))$, respectively, in units of e_σ. Strictly speaking this ligand-field parameter should be written $e'_\sigma = e_\sigma - e_\delta$ [50]. The story is a little more complicated as far as the π-interactions are concerned since it turns out that the de orbitals as well as the dt_2 orbitals both become π-antibonding [22].

We mentioned above that the SCF computation of AOC type directly delivered the KS-DFT orbitals and their orbital energies, which can be used to find the one-electron parameters of the LF. Regarding the two-electron parameters of *R*, the situation is rather different. Whereas the LF one-electron energies were delivered explicitly by the AOC-KS-DFT in a form that might be described as the eigenenergies of the KS orbital energy operator, the two-electron energies are delivered implicitly by a first order computation that keeps the AOC-DFT orbitals invariant (frozen) while providing the expectation values of the KS-DFT energy operator of the two-electron states expressed in a form that corresponds to single Slater determinants in the spin-orbitals of these invariant AOC-KS-DFT orbitals.

The fact that the AOC-DFT computational results must refer to single Slater determinants, which are rarely eigenstates, is the weakness of DFT and this weakness provides LFR with the power of being able to pay something back to the AOC-DFT for its efforts in feeding LFR, and also for its most remarkable ability to mimic the complete LFR model. This model acts on a limited function space, the partially filled shell. Therefore, when setting up the two-electron energy matrix, LFR parameterizes the full matrix, thereby including the non-diagonal elements, which are not accessible by the use of DFT by itself. However, the information in the diagonal elements is more than sufficient to provide the values of the parameters describing *R*, even in the case of the PMT model for which the values of four *R* parameters have to be determined. Once these values are known, they can be used to supplement the AOC-DFT with its lacking non-diagonal elements. Thus, the AOC-DFT model became completed within the LFR regime.

In this way we have seen how we are able to make the two completely independent models, the AOC-KS-DFT computational MO model and the atomic, algebraic, and parametrical LFR model, enter into a loose partnership, which asymmetrically illuminates and supplements both of these models. In the following part of this section we shall extend and deepen this statement, in Section 4.2 with the emphasis on *R* and in Section 4.3 on LF.

4.2. Electron–electron interaction exemplified by LFR analysis of AOC-KS-DFT computational results for CrX_4 of T_d symmetry

Quantitative ligand-field theory is semi-empirical. This means that LFT is atomic in character in the sense that each of its results is expressed as a product of an angular, theoretical factor and a radial, empirical one. All radial factors can alternatively be found computationally by using AOC-DFT, which therefore may be conceived as a pseudo-experimental tool. LFR is LFT whose model Hamiltonian is a sum of only the two major terms, the ligand field and the interelectronic repulsion. In two previous contributions on the use of DFT to mimic LFR, we considered the naked transition metal ions, which means that we handled the *R* part of LFR alone, at first using the SCS two-parameter model [17] and afterwards the PMT four-parameter model [4]. In other words, we considered the electron–electron interaction within idealized d^q configurations.

In the present section, our main issue is again *R*, but this time our systems are tetrahedral complexes. In the treatment of these systems, the ligand-field Hamiltonian is subtracted before the repulsion Hamiltonian is handled.

Each complex CrX_4 (X = F, Cl, Br, I) of T_d symmetry has only one ligand-field parameter, the spectrochemical parameter Δ, which in ligand-field theory may be characterized either as a one-electron parameter or as an orbital-energy parameter. CrX_4 belongs to the simplest molecular systems for the study of the electron–electron interactions in molecular systems. The theoretical part of LFR is atomic in character in the sense that CrX_4, for example, is classified as a d^2 system and the interelectronic repulsion between these two electrons is parametrically described as if the molecule were an atom, that is, had spherical symmetry.

In KS-DFT the many-electron states are defined by use of orbital occupation numbers. For the two-electron states two d spin-orbitals with standard real spatial parts must be attributed the occupation numbers of unity in order to describe a situation that corresponds to a Slater determinant of wave function theory, WFT. Whereas DFT and WFT in general should cover molecular physics in an almost complementary way, which is not easy to compare

conceptually, Kohn-Sham DFT has a conceptual surface in common with molecular orbital theory: the orbitals. Through the population of its orbitals, KS-DFT specifies the one-electron density in the whole volume of the electronic system, and, remarkably, also indirectly the electron–electron interaction. We found this fact hard to believe, and since we had been concerned with electron–electron interactions in LFT [8,9] as well as in its atomic-spectroscopy basis [19b,20], this two-electron content of KS-DFT gave us an impetus for further study [17].

We started out with atoms and with the conventional model for the interelectronic repulsion, so called the Slater–Condon–Shortley model. However, we used an unconventional way of parameterizing the model [17,19b]. The semi-empirical SCS model for d^q configurations was conventionally parameterized by either of two parameter sets: the SCS parameter set $\{F_2, F_4\}$, or the Racah set $\{B, C\}$ that has the advantage of associating one of its parameters B with the energy difference between the states of highest spin-multiplicity whose energetic properties are of special interest because of the ubiquity of metal complexes with the highest spin possible within l^q and because of Hund's first rule which tells that the highest spin multiplicity has the lowest energy. Neither of these parameterizations is associated with orthogonal coefficient operators with the consequence that the DFT-computed information cannot be distributed on the individual R operators. Our main focus in this section is to discuss parameterizations that are useful for analyzing and conceptualizing the energy differences within a d^q configuration as well as the corresponding KS-molecular orbital configuration "d^q" referring to its MO description of the CrX_4 complexes.

In our first paper [17] we quantified the AOC-DFT computational results by using the SCS model associated with the alternative parameter set $\{D, E\}$ whose operators, $Q[D]$ and $Q[E]$ are orthonormal, where the orthogonality [19,53,6,22] means that the parameters can be determined independently and the normality that the values of D and E are directly comparable numerically in the sense that if D is larger than E, then so is its influence upon the splitting of the d^q configuration [17,19b]. In subsequent papers we demonstrated the usefulness of the Parametrical Multiplet Term model, PMT, in connection with the analysis of results for d^q [4,20].

Table 4
Interelectronic repulsion parameters for Cr^{4+} and its four halides. For each system eight sets of parameters are given. The first four lines are of GGA type using the PW91 set of functionals. The next four lines are of LDA type using the VWN set of functionals. Within each set, the first line gives the computed PMT parameters, the second and third lines contain the fitted SCS parameters in the determinant basis and the spin basis, respectively, and the fourth line the SCS parameters obtained by contraction. These SCS parameter values are larger for GGA than for LDA without exception. Note also that convergence was not obtained for CrI_4 in GGA/PW91, which therefore does not occur in the table.

System	Functionals	Repulsion parameterization	$E_{av.}$	D_s	D	D_v	E_1	E	E_0
Cr^{4+}	GGA/PW91	PMT	−0.677	0.671		1.123	0.537		0.805
		SCS db			0.769			0.557	
		SCS sb			0.703			0.546	
		SCS ⊂ PMT			0.838			0.563	
	LDA/VWN	PMT	−0.305	0.775		0.950	0.445		1.334
		SCS db			0.806			0.513	
		SCS sb			0.785			0.477	
		SCS ⊂ PMT			0.828			0.534	
CrF_4	GGA/PW91	PMT	−0.323	0.372		0.653	0.281		0.359
		SCS db			0.422			0.287	
		SCS sb			0.388			0.284	
		SCS ⊂ PMT			0.456			0.289	
	LDA/VWN	PMT	−0.104	0.390		0.500	0.219		0.620
		SCS db			0.409			0.250	
		SCS sb			0.396			0.233	
		SCS ⊂ PMT			0.423			0.259	
$CrCl_4$	GGA/PW91	PMT	−0.236	0.284		0.506	0.209		0.253
		SCS db			0.323			0.213	
		SCS sb			0.297			0.211	
		SCS ⊂ PMT			0.351			0.214	
	LDA/VWN	PMT	−0.068	0.289		0.380	0.156		0.436
		SCS db			0.305			0.178	
		SCS sb			0.295			0.166	
		SCS ⊂ PMT			0.317			0.184	
$CrBr_4$	GGA/PW91	PMT	−0.221	0.270		0.489	0.199		0.243
		SCS db			0.309			0.203	
		SCS sb			0.283			0.201	
		SCS ⊂ PMT			0.336			0.204	
	LDA/VWN	PMT	−0.063	0.280		0.376	0.153		0.431
		SCS db			0.297			0.175	
		SCS sb			0.286			0.163	
		SCS ⊂ PMT			0.309			0.181	
CrI_4	GGA/PW91	PMT	–	–		–	–		–
		SCS	–		–	–		–	–
	LDA/VWN	PMT	−0.053	0.262		0.358	0.142		0.397
		SCS db			0.279			0.162	
		SCS sb			0.268			0.151	
		SCS ⊂ PMT			0.291			0.168	

The PMT model was developed by a more or less collaborative effort between the theoretical physicists and the atomic spectroscopists [54–56] and used by us [20] for the determination of spin–orbit coupling constants of gaseous metal ions on the basis of published atomic J-levels of d^q configurations.

The PMT model can be described by relating it to our parameterization of the SCS model [4]. Considering the configuration d^2, then when $Q[E]$ acts only within the space of the spin triplet states, we denote it $Q[E_1]$, and when it acts only on spin singlet states, we denote it $Q[E_0]$. Similarly, when $Q[D]$ acts only within the singlet space and serves to split the ^{1}S state from the other singlet multiplets, we denote it $Q[D_v]$ where v is the symbol for seniority. $Q[D_v]$ is a seniority separator because ^{1}S has the seniority zero while ^{1}D and ^{1}G have the seniorities of 2. Finally, when $Q[D]$ acts on the whole d^2 configuration to separate the singlets from the triplets, we denote it $Q[D_S]$ (Ref. [4], Table 1).

The PMT model turned out to solve a systematic dilemma which we encountered in our attempt to describe our KS-DFT results for the atomic ions by using the SCS model. We found then that the Coulomb and the exchange functional independently gave computational results that obeyed the SCS model, but they did this in a non-commensurable way in that they gave different values for the SCS parameters D and E, both parameters invariably coming out higher-valued with the Coulomb functional than with the exchange functional. This fact we had to conceive as deficiencies of the KS-DFT results and when it turned out that these deficiencies could be interpreted as "systematic errors" in the computational results, we were willing to go on with this idea [22]. The final results for the atomic ions were that when the PMT model was contracted to regenerate the SCS model, completely well-defined parametric values of D and E were obtained (Table 4). Moreover, the SCS model gave a better agreement with experimental atomic data than did the PMT model itself [4].

The story has an extremely important point [17]. The Slater determinants, whose energies represent the accessible quantities of the KS-DFT model, are all eigenfunctions of S_Z, but when $M_s = 0$, they are in general no longer eigenfunctions of the total spin S^2. This fact would not have been the dream of our wishful thinking. If, however, certain linear combinations of the Slater-determinant energies are used (Ref. [4] Eq. (72)), we obtain in the d^2 case energies corresponding to S^2 eigenfunctions instead, which means more attractive results because the triplets and the singlets are thereby separated and thus the $Q[D]$ and $Q[E]$ subspaces of d^2. The determinant-based (db) and the spin-based (sb) energies give the same values of the PMT parameters, and by contraction, also the same values of the SCS parameters. However, if the adaptation to the SCS model is accomplished by fitting, the D and E parameters come out with different values in db and sb (cf. Table 4 and Ref. [4], Fig. 4).

In Table 4 the average energy of the d^2 configuration and a number of R parameters are given for Cr^{4+} and for the four halides and in Table 5 all the corresponding nephelauxetic ratios for the latter. The values of the parameters show a regular pattern, which looks promising for an analysis of the difference between the GGA and LDA description of "d^{2}" eigenstates. Note especially the regularity in the numbers describing the SCS parameterizations. The

Table 5
Nephelauxetic ratios for all the chromium(IV) halides. These ratios are obtained by dividing each R parameter by the corresponding parameter of Cr^{4+}. It is noteworthy that the values of the formal zero-electron parameter $E_{av.}$, which is not a parameter of LFR, still follow the nephelauxetic series and do this in almost quantitatively the same way as the R parameters.

System	Functionals	Repulsion parameterization	$\beta[E_{av.}]$	$\beta[D_s]$	$\beta[D]$	$\beta[D_v]$	$\beta[E_1]$	$\beta[E]$	$\beta[E_0]$
CrF_4	GGA/PW91	PMT	0.48	0.55		0.58	0.52		0.45
		SCS db		0.55	0.55		0.52	0.52	
		SCS sb			0.55			0.52	
		SCS ⊂ PMT			0.54			0.51	
	LDA/VWN	PMT	0.34	0.50		0.53	0.49		0.46
		SCS db		0.51	0.51		0.49	0.49	
		SCS sb			0.50			0.49	
		SCS ⊂ PMT			0.51			0.49	
$CrCl_4$	GGA/PW91	PMT	0.35	0.42		0.45	0.39		0.31
		SCS db		0.42	0.42		0.38	0.38	
		SCS sb			0.42			0.39	
		SCS ⊂ PMT			0.42			0.38	
	LDA/VWN	PMT	0.22	0.37		0.40	0.35		0.33
		SCS db		0.38	0.38		0.35	0.35	
		SCS sb			0.38			0.35	
		SCS ⊂ PMT			0.38			0.34	
$CrBr_4$	GGA/PW91	PMT	0.33	0.40		0.44	0.37		0.30
		SCS db		0.40	0.40		0.36	0.36	
		SCS sb			0.40			0.37	
		SCS ⊂ PMT			0.40			0.36	
	LDA/VWN	PMT	0.21	0.36		0.40	0.34		0.32
		SCS db		0.37	0.37		0.34	0.34	
		SCS sb			0.36			0.34	
		SCS ⊂ PMT			0.37			0.34	
CrI_4	GGA/PW91	PMT	–	–		–	–		–
		SCS	–	–	–	–	–	–	–
	LDA/VWN	PMT	0.17	0.34		0.38	0.32		0.30
		SCS db		0.35	0.35		0.32	0.32	
		SCS sb			0.34			0.32	
		SCS ⊂ PMT			0.35			0.31	

nephelauxetic series is clearly borne out, even if the differences between the data for the heavy halides were probably expected to be more pronounced.

Note that the parameter $E_{av.}$ is associated with a zero-electron operator and has a well-defined value in a given computation. However, it has entirely different values in GGA and LDA. $E_{av.}$ describes the computed average energy of the 45 determinantal states of d^2 and in LFR thereby the average energy of all the d^2 eigenstates, but the meaning of $E_{av.}$ is not clear in a broader perspective and it is not an empirical parameter of LFR. However, differences between $E_{av.}[M_s = m]$ and $E_{av.}[M_s = m + 1]$ were found to be of D type (spin-pairing energy type) [[17], Appendix]. The values of the Slater parameter F^0 or the Racah parameter A have only mathematical relationships to the other parameters of their classes. They are not useful to include in either experimental or DFT parameter fitting because their coefficient operators are formally neither zero-electron nor two-electron operators.

The determinant-basis and the spin-basis provide KS-DFT energies that can be analysed in LFR by considering the diagonal part of R in the two function bases. In both cases the diagonal part of the PMT matrices are mutually orthogonal (corresponding to the LFR operators being diagonally orthogonal) between the D class operators and the E class operators. This is a conceptual advantage when it comes to contracting the PMT model to become the SCS model because the combined influence of the D class operators on the total SSS can be determined independently of that of the E class. The spin-based operators have the additional advantage that all the standard PMT operators are diagonally orthogonal, which means that all four parameters can be determined independently.

The KS-DFT results for CrX_4 have been analysed taking advantage of this independence and collected together in Table 6. The spin-based LF-PMT-parametrical analysis have been taken to illustrate the contributions from $(SSS)_{LF}$, which are diagonal and associated with the single LF parameter Δ, and the diagonal contributions from $(SSS)_R$, in this case $(SSS)_{PMT}$, which is equal to the sum of the diagonal norm squares of all the four energy matrices. $(SSS)_{PMT}$ is obtained by depriving the total $(SSS)_{KS\text{-}DFT}$ of its LF contents, which is diagonal as a fundamental property of KS-DFT and also as a property of a LF adapted to KS-DFT either in the determinant basis or in the spin basis. By the subtraction of $(SSS)_{LF}$ from $(SSS)_{KS\text{-}DFT}$, LFR has created a parametrical image of the AOC-DFT-computed energy matrix of an hypothetical "molecular atomic ion", whose R energy matrix must be non-diagonal but whose non-diagonal elements are non-accessible for KS-DFT but accessible for LFR. By the 1:1 relationship between KS-DFT and LFR, LFR is now able to provide the non-diagonal terms once its parameters have become known [22]. These terms cannot be obtained from KS-DFT without the use of this indirect path.

The ratio between an operator's diagonal norm square, which is a function-basis dependent quantity, and its total norm square is its degree of diagonality. In the spin-basis these degrees are by symmetry 1, 1/7, 11/35, and 11/105, respectively, for the four standard PMT operators (Ref. [4], Table 25), $Q[D_S]$, $Q[D_v]$, $Q[E_1]$, and $Q[E_0]$. Thus, the operator of Hund's first rule, $Q[D_S]$, is diagonal and that of Hund's second rule $Q[E_1]$, has a degree of diagonality equal to 11/35, which is still considerably larger than the values of the two remaining operators [22]. The parameter D of the SCS model is Jørgensen's spin pairing energy parameter whereas the parameter D_s of the PMT model is the spin-pairing energy parameter of this model and at the same time a parameter of Hund's first rule [59]. E_1 is the parameter of Hund's second rule. More explicit energy expressions can be found in [Ref. [4], Tables 1 and 25]. The norm squares of the standard PMT operators are (280/7), (120/7), (360/7), and (40/7), respectively. It should be noted how clearly the Hund's rule operators dominate the contributions to $(SSS)_{PMT}$. The contributions from the other operators are small even though their parameter values are large. This is caused by the fact that their squared values must be weighed by two comparatively small factors, the norm square of their operators and their degrees of diagonality. For example, the contribution from E_0 of CrF_4 is equal to the parameter factor, equal to $(0.359)^2\ \mu m^{-2}$ according to Table 4, times its norm square (40/7), times its degree of diagonality (11/105), altogether $0.077\ \mu m^{-2}$, which is its diagonal norm square as can be found in Table 6.

AOC-DFT provides numbers of high precision, but they still depend rather much upon the choice of sets of functionals and basis sets for the KS orbitals. However, within a given choice the accuracy of the values of the parameters can be estimated from the usual statistical machinery of the conventional least squares procedure and the agreement with the LFR model is extraordinary good, showing that we now are in possession of a marvelous tool, which is likely to be sharpened as time passes on. The statistical machinery provides E_0 with a relatively high standard deviation in agreement with the fact that $(SSS)_{PMT}$ according to the example is little sensitive to the actual value of E_0.

Table 6
Data from spin-based AOC-DFT computations. For the first three systems, there are for each molecule two computations [57,58], one of GGA type (PW91) and one of LDA type (VWN). The column denoted by $(SSS)_{DFT}$ contains the sum of the squares of the 45 barycentered expectation values. That denoted by $(SSS)_{LF}$ contains the ligand-field contribution to this sum. Column $(SSS)_{DFT\text{-}R}$ contains the AOC-DFT attempt at mimicking the sum square splitting $(SSS)_R$ of the expectation values attributed to the two-electron operators. The following four pairs of columns contain the SSS-contributions of the four two-electron operators together with their percentage contributions to the total $(SSS)_R$. Finally, the residual is the contribution from the AOC-DFT computation that cannot be accounted for by the LF-PMT model and the following column its percentage of $(SSS)_{DFT\text{-}R}$. For CrI_4 the PW91 computation is lacking because of convergence problems with the AOC state, probably because the molecule is close to being unable to exist. However, in the unrestricted use of PW91, convergence was obtained. From Table 7 it is seen that both iodo complexes end up having a monstrous charge transfer to the central atom indicating that the complexes are well on the way towards non-existence.

	$(SSS)_{DFT}$	$(SSS)_{LF}$	$(SSS)_{DFT\text{-}R}$	$(D_{s,norm})^2$	$(D_{s,norm})^2$ (%)	$(D_{v,norm})^2$	$(D_{v,norm})^2$ (%)	$(E_{1,norm})^2$	$(E_{1,norm})^2$ (%)	$(E_{0,norm})^2$	$(E_{0,norm})^2$ (%)	Residual	Residual (%)
CrF_4													
GGA, PW91	25.950	17.977	7.974	5.542	69.499	1.043	13.078	1.279	16.037	0.077	0.966	0.034	0.421
LDA,VWN	28.547	20.819	7.729	6.084	78.719	0.613	7.938	0.776	10.038	0.230	2.975	0.026	0.331
$CrCl_4$													
GGA, PW91	13.581	8.938	4.643	3.228	69.524	0.628	13.526	0.709	15.262	0.038	0.828	0.040	0.860
LDA,VWN	14.192	9.941	4.251	3.349	78.787	0.354	8.336	0.396	9.305	0.114	2.675	0.038	0.898
$CrBr_4$													
GGA, PW91	11.162	6.939	4.223	2.919	69.125	0.586	13.883	0.642	15.205	0.035	0.838	0.040	0.949
LDA,VWN	11.746	7.728	4 .018	3.145	78.278	0.346	8.606	0.380	9.449	0.111	2.763	0.036	0.904
CrI_4													
LDA,VWN	9.334	5.807	3.527	2.705	77.89	0.310	8.880	0.330	9.25	0.090	2.681	0.046	1.304

The square root of the ratio between the norm square of the complete R energy matrix of the imaginary molecular atomic ion and the analogous quantity of the gaseous atomic ion is an accumulative measure of the nephelauxetism of the corresponding molecular system [8–10]. These norm squares both have the SCS and PMT expressions

SCS: $(400/7)(D^2 + E^2)$
PMT: $(280/7)D_S{}^2 + (360/7)E_1{}^2 + (120/7)D_v{}^2 + (40/7)E_0{}^2$

respectively. Note that nephelauxetic ratios are defined as ratios between analogous repulsion parameters referring to the molecular system and to the corresponding gaseous central ion. Because of this definition, these ratios follow the reverse order of the nephelauxetic series. If the PMT formula is used for calculating the accumulative nephelauxetic ratio for CrF_4 using the GGA data from Table 4, this is found to be 0.544, which is not unexpected when a comparison is made with the individual parameter ratios of Table 4.

The relationship between our SCS parameters and the better known Racah parameters are the following [19b]:

$$B = \frac{4}{21}E$$

$$C = \frac{6}{7}D - \frac{10}{21}E$$

where it may be noticed (Tables 4 and 5) that the ratio D/E is almost constant at 1.5 corresponding to the Racah ratio $C/B = 4.25$, which is in agreement with the usual choice in ligand-field contexts, when an experimentally based ratio is lacking.

The contribution of Δ to SSS ($(SSS)_{LF}$, Table 6) is invariably more than 10% higher for the LDA computation than for the GGA one. This contribution is independent of whether the directly obtained M_S-state energies (Slater determinant basis) or the adapted S state energies (spin-basis) are used to calculate it. This independence does not apply to the two-electron contributions. Here the S adaptation gives the higher computed SSS values because it corresponds to a partial diagonalisation of the repulsion matrix. In this context, the differences between the GGA and the LDA parameters are caused mainly by the fact that the two kinds of functional sets produce different metal to ligand distances and thus "different chemical systems".

The ratio $(SSS)_{LF}/(SSS)_{DFT}$ (Table 6) is a measure of how (extremely) molecular all these molecular atomic ions are in the LFR model. This ratio goes for the CrX4 complexes from 68 to 62% for PW91 and from 73 to 62% (here for CrI_4) for VWN down the halide series. The fact that the heavy halides are the least molecular in both series is qualitatively consistent with the finding that the nephelauxetism of CrF4 seems to be overestimated (cf. comment to Table 5) However, the new possibilities of gaining chemical understanding through DFT may not ever allow us to rationalize percentages of that kind because they depend on a comparison of one- and two-electron parameters. One has to remember that LFR parameter values have never been accessible to computation before and what they really mean physically is not quite clear.

4.3. Exemplification of one-to-one connections between AOC-KS-DFT and LFR: bisphenoidally distorted tetrahedral complexes of D_{2d} symmetry

We have seen that there are two levels at which DFT can be held together with and compared with LFR: at the ligand-field orbital level and at the ligand-field Slater determinant level [4]. In this section we exemplify this further by considering the four $VX_4{}^-$ systems, equally angularly distorted and parameterized by the complete set of parameters required by symmetry for the LF-PMT model [21]. This is a case, which from a theoretical point of view is not overparameterized, and which therefore, both in principle and in practice, as we shall see, can be handled computationally, but which never could be handled experimentally. Firstly, geometrical distortions cannot be realized experimentally, and secondly, there has hardly ever been an experimental situation of this type where more than four or five relevant energies have with certainty been identified for a given chemical system.

The connections between DFT and LFR are found by looking at the symmetry species and their standard components; for example, when focusing at the orbitals of the partially filled shell, one finds exactly one orbital labeled t_2xy in the DFT class and one in the LFR class, where the component label xy is the connecting label when the symmetry is lowered [22]. This label refers to the real standard d orbital that was used on a neat symmetry basis to define the particular component of the symmetry species $t_2(T_d)$. The orbital symmetry referring back to the same d orbital [21] in the case of a molecular symmetry D_{2d} is denoted by $b_2xy(D_{2d})$ when given its full label. The example can be directly extrapolated to the remaining four real standard d orbitals. A full label is often not required because it is clearly understood from the context. On the other hand, many of the mistakes or misunderstandings in the literature have arisen from unclear or insufficient symbols. The most prominent example is the identical notation of symmetry species belonging to different groups in which case the specification of the relevant group, as exemplified right above, is a necessity unless it is absolutely clear from the context.

The component story can easily be transferred from the orbital level to the Slater-determinant level [21,22]. There is, for example, one ligand-field Slater determinant of the type $|t_2(xy)^+t_2(yz)^-|$ in both models. Therefore, the immediate conclusion is that the one-to-one relationship that exists between the orbitals also applies to the ligand-field Slater determinants of the two models.

Again, the AOC-KS-DFT model provides the Slater determinant energies and the LFR model the parameters, but now in terms of linear combinations of ligand-field parameters and repulsion parameters. A set of 45 linear equations is the consequence, and LF as well as R parameter values can be obtained as a result of solving these equations. Often the number of equations exceeds the number of parameters in which case standard deviations can be obtained by application of the least squares fitting procedure and the standard statistical machinery [17,21,22].

In Fig. 6 we have graphically produced the results for tetragonally distorted tetrahedral halide complexes of V^{III}. The AOM-PMT model has been used to determine three linearly independent AOM parameters, which is the number predicted by the holistic ligand-field model for a complete description of all the "d" KS molecular orbital energy differences in the case of the point group D_{2d}. Under these circumstances conceptually meaningless, but numerically meaningful, standard deviations on the AOM parameters are obtained. The variances must instead refer to R rather than to LF. This is a consequence of the completeness of LF and the orthogonality of LF and R and the machinery cannot know that.

For regular tetrahedral symmetry, the monatomic ligands are by symmetry effectively linearly ligating and the same is true for infinitesimal distortions of the tetrahedron (cf. the vibronic equations of Section 3.4), but for such a large distortion as that used here, the fact that the two π-parameters come out with the same values is a rather strong support to the usual linear-ligation assumption of the AOM, especially in view of the fact that this assumption will become more and more absurd as the angular distances between the ligands approach zero.

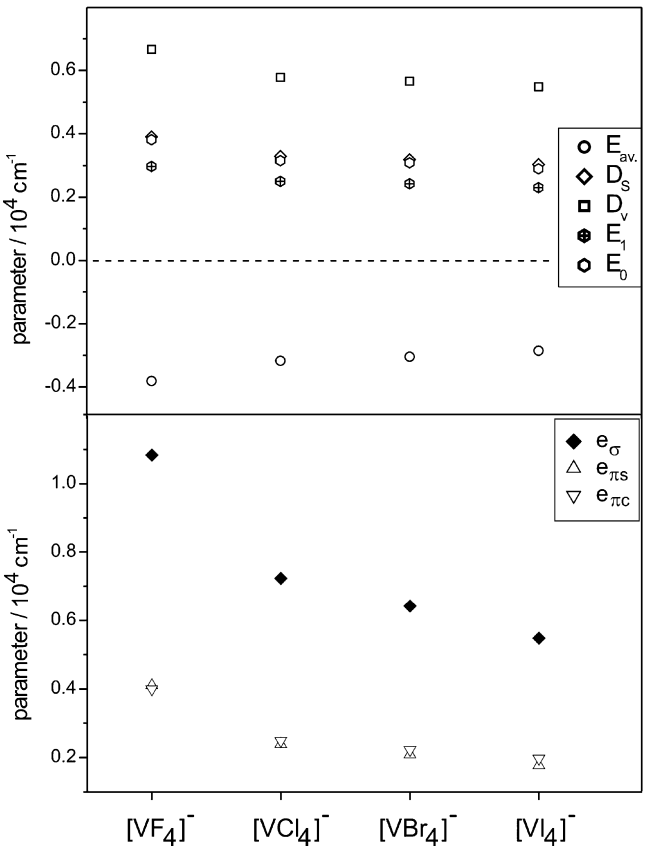

Fig. 6. AOC-DFT computation of Slater-determinant states of tetragonal vanadium(III) halide complexes. Their geometries are bisphenoidally compressed tetrahedral with the top and bottom valence angles equal to 120°. Their point group is D_{2d}. The computational results have been used to mimic LFR where LF has been parameterized by a complete set of AOM parameters, which by the fact that the two π parameters have obtained the same values (within their standard deviations) supports the conventional assumption about linear ligation of monatomic ligands. Moreover, the results illustrate the general fact that the σ parameters are a little more than three times as large as the π parameters. The *R*-part of LFR has been parameterized by the PMT model for d^2. The parameters D_S and E_1 are the parameters of Hund's first and second rule, respectively. Although these parameters are the numerically smaller ones of each set, they are in combination with their associated operators the energetically dominating (cf. Table 6). The order of the values of the PMT parameters is invariably $D_v \gg D_S > E_0 \gg E_1$ .The chemical results can be embraced by the pictorial expression F ⋙ Cl > Br ≫ I.

4.4. Quantitative ligand-field theory: history and outlook

We emphasized in the introduction to this review that LFT is an old structure of immense ability of survival. In the 1930s it was considered to be a physical model of the magnetic properties of transition metal complexes ending up with Van Vleck's attempt at understanding the d–d absorption spectra. His idea was far reaching, but at that time did not reach any further than to the spin-forbidden transitions of chromium alum. With his experimental bank as a background, he had to conceive the spin-allowed bands as absorption edges.

In the 1940s LFT slept. In the 1950s, the physicists had almost lost their interest in the subject, and the subject had been rediscovered by a chemist in the ruins of Frankfurt. Ilse produced a thesis in 1946 [60] where both weak-field and strong-field approaches to LFT were developed, and both ionic and dipolar ligands were treated. Ilse had died before the first communication from Frankfurt [61] became public in the weak-field formulation and from Oxford [62] in the strong-field formulation. In 1954 came from Tokyo [63] the physicists' major contribution from that time by the publishing of energy matrices of cubic complexes of all the d^q configurations, and Copenhagen [64] came along with a chemical weight that was catalysed by a several generation long experimental tradition. Soon after, Cambridge [65] joined the ligand-field work by adding valuable contributions based upon a special mathematical insight. Two generations of Japanese chemists had photographed solution spectra from Werner's time and had discovered the spectrochemical series when they began the measurements of polarized spectra, and Yamatera [66a,66b] laid the foundation to the angular overlap model [66c] as did McClure [67]. Jørgensen, Pappalardo and Schmidtke made a major step [68] before more actors joined the scene. Then, for more than 5 years, LFT was in the forefront of inorganic science, and when the light upon the subject seemed to fade, the AOM gradually became fully developed [49–52,70].

Since then, the intensity of interest in LFT has been coming and going depending on the various physical techniques that needed explanatory modeling where LFT could be used.

At the present time, perhaps the most important physical technique is KS-DFT, which we have discussed in this review in relation to LFT. As to quantitative LFR, we have only discussed the very simplest problems where symmetry could be used to predict the number of parameters of the LF and where the PMT model could be used to parameterize *R* (cf. Tables 4–6 and Fig. 6).

The functioning of the one-to-one relationship between the molecular AOC-KS-DFT and the atomic LFR has been remarkable. However, we have only transported energies on that account. In an outlook from where we stand at this time, one would certainly see a further clarification of why the encounter between these two incommensurable models was so successful.

In agreement with chemical intuition, the more ionic bonding in the fluoride complexes is reflected in the metal charge (cf. the last column of Table 7), which is ca. one unit larger for the fluoride complexes as compared to the other halide complexes. Quite generally, the charge transfer into the d orbitals is much more pronounced than that into the s and p orbitals. This applies in particular to the fluoride complexes.

In general, the covalency of the halides increase dramatically with the formal charge of the central ion. This behaviour is so pronounced that the Mulliken charge on Cr^{IV} is lower than on V^{III}. However, the less polarizable fluoride constitutes an exception where the s and p covalency decreases on going from V^{III} to Cr^{IV}. This may be related to the higher central ion charge in the fluoride complexes and the concomitant more hydrogen-like orbitals, which leave the 4s and 4p orbitals energetically more isolated.

We need to mention that the Mulliken charge is based upon the equal sharing of the overlap charge between the two ends of a bond. This arbitrary choice of sharing is not only basis dependent, but clearly also the more convincing the more homopolar the bond is. Therefore, we have communicated the above AOC-DFT-computational results with some reservation at least as far as their quantitative truth is concerned.

We observe as in Section 3, but yet to our surprise, that chloride is consistently computed to result in more covalent complexes than bromide except when one focuses upon the transfer into the metal d orbitals, where the usual order of the two halides is equally consistently found, in agreement with the spectroscopic evidence of Tables 4–6.

5. LFT and DFT symbiosis in the future – conclusions

As the standard tool for rationalizing and systematizing transition metal chemistry, LFT has had an important historical role, which is likely to persist. With chemists synthesizing and modeling increasingly more complex systems, the theoretical descriptions

Table 7
l-Dependent partitioning of the charge transfer arising in the bonding process.

		s	p	d	f	d/(s+p+d+f)	s+p+d+f	3-(s+p+d+f)
GGA	VF_4^-	0.08	0.23	1.17	0.05	0.76	1.54	1.46
	VCl_4^-	0.24	0.52	1.59	0.03	0.67	2.37	0.63
	VBr_4^-	0.20	0.41	1.59	0.02	0.72	2.22	0.78
	VI_4^-	0.43	0.78	1.91	0.02	0.61	3.14	−0.14
LDA	VCl_4^-	0.25	0.53	1.68	0.03	0.67	2.49	0.51
		s	p	d	f	d/(s+p+d+f)	s+p+d+f	4-(s+p+d+f)
GGA	CrF_4	0.03	0.17	1.98	0.06	0.88	2.24	1.76
	$CrCl_4$	0.28	0.70	2.61	0.03	0.72	3.63	0.37
	$CrBr_4$	0.22	0.56	2.66	0.02	0.77	3.46	0.54
LDA	CrF_4	0.03	0.15	2.10	0.07	0.89	2.35	1.65
	$CrCl_4$	0.35	0.81	2.76	0.04	0.70	3.95	0.05
	$CrBr_4$	0.31	0.73	2.79	0.02	0.72	3.86	0.14
	CrI_4	0.64	1.12	3.19	0.02	0.64	4.97	−0.97

are simultaneously increasing in complexity and loosing in generality. In order to guide chemical intuition and develop broad understanding of coordination chemistry, the simplicity and broadness of scope of LFT makes it well suited as a framework for the analysis and simplification of current molecular orbital calculations and as such a tool of continued relevance to the coordination chemist. In the preceding sections, we have reviewed our work on the use of KS-DFT to revive ligand-field theory. As we see it, KS-DFT has a qualitative and a quantitative application both of which serve as supplements to experiments.

Those quantitative applications which focus directly upon LFT, and which therefore have to use invariant (frozen) orbitals, must be based upon a somehow constrained use of KS-DFT. We have used the average of configuration DFT (AOC-DFT), which addresses what we have called atomic ligand-field theory. This description is a strictly defined mathematical framework including a sum of products of angular and radial factors, where the angular ones embodies the symmetry- or geometry-exact properties, and the radial ones quantify the magnitude of the ligand field, which in this context encompasses the energy parameters of the ligand field itself as well as the effective interelectronic repulsion. This type of quantitative mimicking of LFT has up until now not been used by more than a few workers, notably Atanasov and Daul with their LFDFT approach [18,69]. These authors have tried to place LFDFT within a broader and more flexible theoretical scheme while we have focussed upon analysing details within the strictly atomic theoretical framework.

The goal of bridging quantitatively between DFT computations and LFT descriptions can, as shown in this paper, be approached by two rather different philosophies, one focussing only on the one-electron operator part of LFT and another encompassing both ligand field and interelectronic repulsion. In the first of these approaches DFT is used in a straightforward manner to provide a description which is optimal within its own realm. Here focus is on orbital energies (orbital splittings) and the correspondence established between DFT and LFT is confined to the description of the ligand field in the two models. This approach constitutes the simplest mapping of DFT results onto LFT and is limited in methodological freedom. Projecting LFT descriptions out of DFT results for d^1 systems is, thus, straightforward and the possible variations lie within the treatment of covalency, *l*-mixing and energies of virtual orbitals. The primary advantages of this approach are that it is simple and faithful towards the DFT description by imposing no LF-derived conditions on the DFT data. In combination with a suitable choice of parameterization for the one-electron part of the LF-Hamiltonian, this approach can, as illustrated in Section 3, make the full machinery of orthogonal ligand-field parameterizations applicable to DFT results and aid the interpretation of these in terms of symmetry hierarchies. With chemically based parameterizations such as that of the AOM, the general problem of over-parameterization in the ligand-field description, however, remains an important problem in the process of mapping DFT onto LFT. The advantage of computational chemistry that all energies and coupling strengths are accessible led in Section 3 to a quite general solution to this problem of over-parameterization. It was demonstrated how "in silico" experiments render vibronic-coupling (VC) constants "experimentally accessible" entities with parametrical expressions of the AOM which are independent of the AOM energy expressions for the d orbitals, and which in general reduce the problem with the data to parameter ratio in AOM-LFT models.

This DFT-LFT-VC method is not confined to one-electron systems as is demonstrated in Section 4.3 where its application to furnish AOM parameters for tetrahedral d^2 systems was reviewed. While this method thus bridges between our discussions of one- and many-electron systems, there remains a philosophical as well as a practical barrier between Sections 3 and 4. When DFT is used to model systems with more than one electron in an open *l*-shell, the different nature of DFT and LFT necessitates some adaptation of the way in which the DFT model is applied. The common function basis of a strong-field limit of LFR and a Slater determinant analog of KS-DFT constitutes the desired bridge between the models, but whereas LFR treats all states of a full d^q configuration as a whole, KS-DFT normally deals with a specific state defined by occupations of SCF KS-orbitals. The similarity in function basis is therefore only apparent if DFT is used unconstrained with the different strong-field many-electron determinants, built from different sets of orbitals. To make the two descriptions genuinely share their many-electron function basis, this basis has to be built from a single set of orbitals. This constraint on the DFT modeling is built in via the average-of-configuration calculation, which in order to mimic the LFT description has to be a spin-restricted calculation. The undesirable, but unavoidable consequence is that the bridge to LFR is established at the cost of introducing a discontinuity in the way DFT is applied.

At present, the best solution appears to be the use of a spin-unrestricted geometry optimization by DFT whereupon a spin-restricted AOC calculation defines the one-electron function basis whose partially filled Kohn-Sham MO shell "d^q" has a one-to-one correspondence with the d^q shell of LFR. The analogous way in which the two models build up their many electron state functions secures that the one-to-one correspondence applies to the *q*-electron states as well. However, since DFT is based upon the one-electron density distribution and KS-DFT on the specification

of this distribution by occupation numbers of KS orbitals, it seems like a little miracle that these orbitals are able to support a model including effective two-electron operators.

A brief summary of the approaches of Atanasov coworkers [18a–d] and of us [4,17,22] is justified by the fact that the LFDFT model and ours are identical as far as the use of AOC-DFT and the Amsterdam Density Functional [70] package is concerned; even as far as the purpose of obtaining the complete set of d^q eigenstates. There is an essential difference, however. We use a formulation of LFT based upon coefficient operators that are mutually orthogonal wherever possible [4,19]. This formulation allows us to choose Jørgensen's spin-pairing energy parameter *D*, which separates the KS-DFT Slater-determinants into three main classes, in combination with Racah's parameter *B*, which takes care of their sub-classes [17]. Moreover, each of these parameters can be supplemented [4,20] by minor complementary ones, which leave us with an almost indispensable tool for describing the deviations of the AOC-DFT results from the SCS model [4]. The obtained parametrical results are dependent on the choice of parameterization due to fixation of the function basis by KS-DFT. Accordingly, since only the diagonal part of the operators in a strong-field basis are used, different choices of repulsion parameterization spanning the same operator basis may reproduce experimental data differently.

Finally, we see the developments within quantitative LFT, which mathematically is an atomic model, as independent of those of KS-DFT, which is molecular in character, and we find mutual illumination of the two models a better philosophy than unification.

Our use of DFT to illuminate LFR has all the time had one direction. We used DFT to provide information that corresponds to the empirical part of the semi-empirical LFR. However, the one-to-one strong-field correspondence, in spite of the spin symmetry breaking dictated by the Slater determinant requirement of KS-DFT, immediately suggested a mutual relationship and a possible synergistic relationship between the two models, namely, that the DFT-unattainable non-diagonal elements of the LFR through the known values of its parameters could be reflected back to the DFT.

References

[1] (a) J.C. Slater, Phys. Rev. 37 (1931) 481;
(b) L. Pauling, J. Am. Chem. Soc. 53 (1931) 1367.
[2] (a) J.C. Slater, Phys. Rev. 34 (1929) 1293;
(b) E.U. Condon, G.H. Shortley, The Theory of Atomic Spectra, 1st ed., Cambridge University Press, Cambridge, UK, 1935.
[3] (a) J. Bendix, C.E. Schäffer, M. Brorson, Coord. Chem. Rev. 94 (1989) 181;
(b) M. Brorson, G.S. Jensen, C.E. Schäffer, J. Chem. Ed. 63 (1986) 387.
[4] C. Anthon, J. Bendix, C.E. Schäffer, Struct. Bond. 107 (2004) 207.
[5] e.g;
(a) K.E. Purcell, J.C. Kotz, Inorganic Chemistry, W.B. Saunders, Philadelphia, USA, 1977;
(b) J.E. Huheey, Inorganic Chemistry, 3rd ed., Harper International, Cambridge, UK, 1983;
(c) F.A. Cotton, G. Wilkinson, Advanced Inorganic Chemistry, 5th ed., Wiley Interscience, NY, 1988;
(d) C. Housecroft, A.G. Sharpe, Inorganic Chemistry, 3rd ed., Pearson, Essex, UK, 2008.
[6] J. Bendix, M. Brorson, C.E. Schäffer, ACS Symp. Ser. 565 (1994) 213.
[7] (a) F. Neese, J. Biol. Inorg. Chem. 11 (2006) 702;
(b) J.C.A. Boyens, J.F. Ogilvie (Eds.), Models, Mysteries and Magic of Molecules, Springer, 2007, p. 411.
[8] C.E. Schäffer, C.K. Jørgensen, J. Inorg. Nucl. Chem. 8 (1958) 143.
[9] C.E. Schäffer, J. Inorg. Nucl. Chem. 8 (1958) 149.
[10] (a) C.K. Jørgensen, Prog. Inorg. Chem. 4 (1962) 73;
(b) C.E. Schäffer, Inorg. Chim. Acta 300–302 (2000) 1035.
[11] (a) J.H. Van Vleck, J. Chem. Phys. 3 (1935) 803;
(b) J.H. Van Vleck, J. Chem. Phys. 3 (1935) 807.
[12] R.J. Deeth, Dalton Trans. (1991) 1467.
[13] T. Ziegler, A. Rauk, E.J. Baerends, Theor. Chim. Acta 43 (1977) 261.
[14] (a) C. Daul, Int. J. Quant. Chem. 52 (1994) 867;
(b) C. Daul, A. Goursot, Int. J. Quant. Chem. 29 (1986) 779.
[15] (a) F. Gilardoni, J. Weber, K. Bellafrouh, C. Daul, H.-U. Güdel, J. Chem. Phys. 104 (1996) 7624;
(b) K. Doclo, D. De Corte, C. Daul, H.-U. Güdel, Inorg. Chem. 37 (1998) 3842;
(c) J.A. Aramburu, M. Moreno, K. Doclo, C. Daul, M.T. Barriuso, J. Chem. Phys. 110 (1999) 1497;
(d) A. Borel, L. Helm, C.A.E. Daul, Chem. Phys. Lett. 383 (2004) 584;
(e) A. Borel, C.A. Daul, J. Mol. Struct.: THEOCHEM 762 (2006) 93.
[16] E.J. Baerends, V. Branchadell, M. Sodupe, Chem. Phys. Lett. 265 (1997) 481.
[17] C. Anthon, C.E. Schäffer, Coord. Chem. Rev. 226 (2002) 17.
[18] (a) M. Atanasov, C.A. Daul, C. Rauzy, Chem. Phys. Lett. 367 (2002) 737;
(b) M. Atanasov, C.A. Daul, C. Rauzy, Struct. Bond. 106 (2004) 97;
(c) M. Atanasov, C.A. Daul, Comptes Rend. Chim. 8 (2005) 1421;
(d) M. Atanasov, C. Daul, H.-U. Gudel, T.A. Wesolowski, M. Zbiri, Inorg. Chem. 44 (2005) 2954;
(e) M. Atanasov, C. Rauzy, P. Baettig, C. Daul, Int. J. Quant. Chem. 102 (2005) 119.
[19] (a) C.E. Schäffer, Physica A 114 (1982) 28;
(b) M. Brorson, C.E. Schäffer, Inorg. Chem. 27 (1988) 2522.
[20] J. Bendix, M. Brorson, C.E. Schaffer, Inorg. Chem. 32 (1993) 2838.
[21] C. Anthon, J. Bendix, C.E. Schäffer, Inorg. Chem. 43 (2004) 7882.
[22] C. Anthon, J. Bendix, C.E. Schäffer, Inorg. Chem. 42 (2003) 4088.
[23] S.I. Arshankow, A.L. Poznjak, Z. Anorg. Allg. Chem. 481 (1981) 201.
[24] (a) J.W. Buchler, C. Dreher, K.-L. Lay, Z. Naturforsch. B 37 (1982) 1155;
(b) J.W. Buchler, C. Dreher, K.-L. Lay, Y.J.A. Lee, W.R. Scheidt, Inorg. Chem. 22 (1983) 888.
[25] H. Grunewald, H. Homborg, Z. Anorg. Allg. Chem. 608 (1992) 81.
[26] J. Du Bois, J. Hong, E.M. Carreira, M.W. Day, J. Am. Chem. Soc. 118 (1996) 915.
[27] A. Niemann, U. Bossek, G. Haselhorst, K. Wieghardt, B. Nuber, Inorg. Chem. 35 (1996) 906.
[28] K. Meyer, J. Bendix, N. Metzler-Nolte, T. Weyhermueller, K. Wieghardt, J. Am. Chem. Soc. 120 (1998) 7260.
[29] K. Meyer, J. Bendix, E. Bill, T. Weyhermueller, K. Wieghardt, Inorg. Chem. 37 (1998) 5180.
[30] J. Bendix, R.J. Deeth, T. Weyhermueller, E. Bill, K. Wieghardt, Inorg. Chem. 39 (2000) 930.
[31] J. Bendix, K. Meyer, T. Weyhermueller, E. Bill, N. Metzler-Nolte, K. Wieghardt, Inorg. Chem. 37 (1998) 1767.
[32] J. Bendix, T. Birk, T. Weyhermuller, Dalton Trans. (2005) 2737.
[33] J. Bendix, J. Am. Chem. Soc. 125 (2003) 13348.
[34] B. Moubaraki, K.S. Murray, P.J. Nicols, S. Thomson, B.O. West, Polyhedron 13 (1994) 485.
[35] (a) L. Kervan, J. Phys. Chem. 88 (1984) 327;
(b) C.J. Ballhausen, B.F. Djurinskij, K.J. Watson, J. Am. Chem. Soc. 90 (1968) 3305.
[36] U. Müller, I. Lorentz, Z. Anorg. Allg. Chem. 463 (1980) 110.
[37] D. Bright, J.A. Ibers, Inorg. Chem. 8 (1969) 709.
[38] U. Schubert, E. Neugebauer, P. Hofmann, B.E.R. Schilling, H. Fischer, A. Motsch, Chem. Ber. 114 (1981) 3349.
[39] K. Wieghardt, G. Backes-Dahmann, W. Holtzbach, W.J. Swiridoff, J. Weiss, Z. Anorg. Allg. Chem. 499 (1983) 44.
[40] M. Carrondo, R. Shakir, A.C. Skapski, Dalton Trans. (1978) 844.
[41] C.-M. Che, M.H.-W. Lam, T.C.W. Mak, Chem. Commun. (1989) 1529.
[42] (a) C.E. Schäffer, Inorg. Chim. Acta 240 (1995) 581, references therein;
(b) M.J. Riley, Inorg. Chim. Acta 268 (1998) 55;
(c) D. Reinen, M. Atanasov, Struct. Bond. 107 (2004) 159.
[43] (a) D.W. Smith, Inorg. Chim. Acta 22 (1977) 107;
(b) L. Falvello, M. Gerloch, Inorg. Chem. 19 (1980) 472;
(c) R.J. Deeth, Faraday Discuss. 124 (2003) 379;
(d) E. Tangen, J. Conradie, A. Ghosh, J. Chem. Theory Comput. 3 (2007) 448;
(e) L.E. Orgel, An Introduction to Transition Metal Chemistry, Methuen, London, 1960;
(f) C.E. Schäffer, Inorg. Chim. Acta 240 (1995) 581–592;
(g) M.J. Riley, Inorg. Chim. Acta 268 (1998) 55–62.
[44] (a) J. Bendix, A. Bogevig, Inorg. Chem. 37 (1998) 5992;
(b) J. Bendix, H. Birkedal, A. Bogevig, Inorg. Chem. 36 (1997) 2702, references therein;
(c) H.J. van der Westhuizen, S.S. Basson, J.G. Leipoldt, W. Purcell, Transition Met. Chem. 19 (1984) 582.
[45] (a) V. Bachler, J. Comp. Chem. 26 (2005) 532;
(b) P. Spuhler, M. Lein, G. Frenking, Z. Anorg. Allg. Chem. 629 (2003) 803.
[46] (a) P. Hummel, J.R. Winkler, H.B. Gray, Theor. Chem. Acc. 119 (2008) 35;
(b) P. Hummel, H.B. Gray, Coord. Chem. Rev. 251 (2007) 554.
[47] (a) M. Bacci, J. Phys. Chem. Solids 41 (1980) 1267;
(b) M. Bacci, Chem. Phys. Lett. 58 (1978) 537;
(c) M. Bacci, Chem. Phys. 40 (1979) 237;
(d) M. Atanasov, P. Comba, C.A. Daul, J. Phys. Chem. A 110 (2006) 13332;
(e) M. Atanasov, P. Comba, C.A. Daul, Inorg. Chem. 47 (2008) 2449.
[48] C.E. Schäffer, Theor. Chim. Acta 34 (1974) 237.
[49] C.E. Schäffer, in: W.C. Price, S.S. Chissick, T. Ravensdale (Eds.), Wave Mechanics—The First 50 Years, Butterworths, London, 1973, p. 174 (Chap. 12).
[50] C.E. Schäffer, Struct. Bond. 14 (1973) 69.
[51] (a) C.E. Schäffer, C.K. Jørgensen, Mol. Phys. 9 (1965) 401;
(b) C.E. Schäffer, C.K. Jørgensen, Mat. Fys. Medd. Dan. Vid. Selsk. 34 (1965) 13.
[52] C.E. Schäffer, Struct. Bond. 5 (1968) 68.
[53] M. Brorson, T. Damhus, C.E. Schäffer, Comm. Inorg.Chem. 3 (1983) 1.
[54] B.R. Judd, R.C. Leavitt, J. Phys. B: Atom. Mol. Phys. 19 (1986) 485.
[55] P.H.M. Uylings, J. Phys. B: Atom. Mol. Phys. 17 (1984) 2375.
[56] J.E. Hansen, B.R. Judd, J. Phys. B: Atom. Mol. Phys. 18 (1985) 2327.
[57] J.P. Perdew, J.A. Chevary, S.H. Vosko, K.A. Jackson, M.R. Pederson, D.J. Singh, C. Fiolhais, Phys. Rev. B: Condens. Matter Mater. Phys. 46 (1992) 6671.

[58] S.H. Vosko, L. Wilk, L. Nusair, Can. J. Phys. 58 (1980) 1200.
[59] F. Hund, Z. Phys. 33 (1925) 345.
[60] F.E. Ilse, Dissertation Frankfurt am Main, 1946.
[61] (a) F.E. Ilse, H. Hartmann, Z. Phys. Chem. 197 (1951) 239;
(b) F.E. Ilse, H. Hartmann, Z. Naturforsch. 6a (1951) 751;
(c) H. Hartmann, H.L. Schläfer, Z. Naturforsch. 6a (1951) 760.
[62] (a) L.E. Orgel, J. Chem. Soc. (1952) 4756;
(b) L.E. Orgel, J. Chem. Phys. 23 (1955) 1004.
[63] Y. Tanabe, S. Sugano, J. Phys. Soc. Jpn. 9 (1954) 753.
[64] (a) J. Bjerrum, C.J. Ballhausen, C.K. Jørgensen, Acta Chem. Scand. 8 (1954) 1275;
(b) C.J. Ballhausen, Mater. Fys. Medd. Dan. Vid. Selsk. 29 (4) (1954);
(c) C.J. Ballhausen, Mater. Fys. Medd. Dan. Vid. Selsk. 29 (8) (1954);
(d) C.K. Jørgensen, Acta Chem. Scand. 8 (1954) 1502;
(e) C.K. Jørgensen, Acta Chem. Scand. 9 (1955) 116;
(f) C.J. Ballhausen, C.K. Jørgensen, Acta Chem. Scand. 9 (1955) 397;
(g) C.J. Ballhausen, C.K. Jørgensen, Mater. Fys. Medd. Dan. Vid. Selsk. 29 (14) (1955);
(h) C.K. Jørgensen, Acta Chem. Scand. 9 (1955) 405;
(i) C.J. Ballhausen, Acta Chem. Scand. 9 (1955) 821.
[65] J.S. Griffith, L.E. Orgel, J. Chem. Soc. (1956) 4981.
[66] (a) H. Yamatera, Naturwissenschaften 44 (1957) 375;
(b) H. Yamatera, Bull. Chem. Soc. Jpn. 31 (1958) 95;
(c) C.E. Schäffer, Pure Appl. Chem. 24 (1970) 361.
[67] D.S. McClure, in: S. Kirschner (Ed.), Proc. VI ICCC. Advances in the Chemistry of the Coordination Compounds, Macmillan, New York, 1961, p. 498.
[68] C.K. Jørgensen, R. Pappalardo, H.-H. Schmidtke, J. Chem. Phys. 39 (1963) 1422.
[69] (a) M. Atanasov, C.A. Daul, E.P. Fowe, Monartshefte f. Chem. 136 (2005) 925;
(b) M. Atanasov, C. Rauzy, P. Baettig, C. Daul, Int. J. Quant. Chem. 102 (2005) 119.
[70] All DFT computations were performed using the ADF program package: G. Velde, E.J. Baerends, Comput. Phys. 99 (1992) 84.